Finite size properties of staggered $U_q[sl(2|1)]$ superspin chains

Holger Frahm[1] and Márcio J. Martins[2]

[1]*Institut für Theoretische Physik, Leibniz Universität Hannover,*
Appelstraße 2, 30167 Hannover, Germany

[2]*Departamento de Física, Universidade Federal de São Carlos,*
C.P. 676, 13565-905 São Carlos (SP), Brazil

(Dated: February 4, 2011)

Based on the exact solution of the eigenvalue problem for the $U_q[sl(2|1)]$ vertex model built from alternating 3-dimensional fundamental and dual representations by means of the algebraic Bethe ansatz we investigate the ground state and low energy excitations of the corresponding mixed superspin chain for deformation parameter $q = \exp(-i\gamma/2)$. The model has a line of critical points with central charge $c = 0$ and continua of conformal dimensions grouped into sectors with γ-dependent lower edges for $0 \leq \gamma < \pi/2$. The finite size scaling behaviour is consistent with a low energy effective theory consisting of one compact and one non-compact bosonic degree of freedom. In the 'ferromagnetic' regime $\pi < \gamma \leq 2\pi$ the critical theory has $c = -1$ with exponents varying continuously with the deformation parameter. Spin and charge degrees of freedom are separated in the finite size spectrum which coincides with that of the $U_q[osp(2|2)]$ spin chain. In the intermediate regime $\pi/2 < \gamma < \pi$ the finite size scaling of the ground state energy depends on the deformation parameter.

I. INTRODUCTION

Studies of exactly solvable two-dimensional vertex models or the equivalent $(1+1)$-dimensional quantum spin chains can provide important insights into the nature of excitations in strongly correlated systems and their critical behaviour. Over the years this approach has provided much to the present understanding of such models based on ordinary Lie algebras whose massless regime is believed to be described by Wess-Zumino-Witten models on the corresponding group. On the other hand, many of the physical properties of vertex models based on Lie *super*algebras and their quantum deformations are still not understood in detail. At the same time and in spite of significant progress in recent years only little is known about the likely candidates for the low energy effective description of these vertex models, i.e. $(1 + 1)$-dimensional conformal field theories with non-compact target spaces. Advances in this direction are highly desirable as they would likely lead to progress for some problems related to the duality between gauge and string theories (see Ref. 1 and References therein) but also in statistical mechanics, e.g. for the description of disorder

driven phase transitions within the superspin approach to non-interacting electron systems, see e.g. [2, 3].

One possible approach to this problem is based on the observation that a non-compact continuum limit can arise from lattice models with a finite number of states per site [4–6]. If such models are integrable the powerful techniques of the quantum inverse scattering method allow for a detailed analysis of their spectrum and ultimately provide important insights into their continuum limit. Concerning the possible applications mentioned above lattice models with alternation between conjugate representations of the superalgebra have been found to be particular important. For the integrable $sl(2|1)$ superspin chain mixing the fundamental representation 3 and its dual $\bar{3}$ this approach has led to the identification of the continuum limit with the $SU(2|1)$ WZW model at level $k = 1$ [4]. Recently, this has been generalized to find the scattering theory arising in the continuum limit of the antiferromagnetic $gl(n + N|N)$ spin chains with $n, N > 0$ [7].

Another direction in which these results may be generalized is by deformation of the underlying symmetry: in the case of ordinary Lie algebras this has led to models which exhibit critical lines with anomalous exponents depending continuously on the deformation parameter. Whether such a behaviour occurs in superspin chains when a deformation parameter is introduced and even whether the critical behaviour of the mixed superspin chain observed in the undeformed case is robust against the deformation is the question which we want to address in this paper.

Our paper is organized as follows: below we recall the definition of the mixed $U_q[sl(2|1)]$ vertex model [8] from which we obtain the integrable superspin Hamiltonian which is then solved by means of the algebraic Bethe ansatz. Since the analysis of the Bethe equations makes use of the known properties of the Fateev Zamolodchikov model [9] with twisted boundary conditions we also summarize what is known about the different critical phases of the latter. In Section IV we present our results on the low energy properties of the mixed superspin chain in the 'antiferromagnetic' regime which can be interpreted as a regularization of a continuum theory consisting of a compact and a non-compact boson, similarly to the $sl(2|1)$ mixed superspin chain discussed in Ref. 4. The critical behaviour in the 'ferromagnetic' regime discussed in Section V turns out to be very different: the corresponding low energy theory exhibits exact spin-charge separation for all values of the deformation parameter q. Both the spinon and the holon modes are described by $U(1)$ Gaussian theories. In the isotropic limit restoring $sl(2|1)$ invariance the spin part of the spectrum acquires a quadratic dispersion above an (completely polarized) reference state while the charge part of the spectrum remains conformal in the same universality class as the isotropic $osp(2|2)$ spin chain [5, 10, 11].

II. MIXED VERTEX MODEL

The weights of the mixed vertex model are based on the R-matrices associated to the three dimensional vector representation of $U_q[sl(2|1)]$ and its dual, labelled 3 and $\bar{3}$ in the following. These R-matrices act on the tensor products $3 \otimes 3$, $3 \otimes \bar{3}$, $\bar{3} \otimes 3$ and $\bar{3} \otimes \bar{3}$ and we shall denote them by $R^{(33)}(\lambda)$, $R^{(3\bar{3})}(\lambda)$, $R^{(\bar{3},3)}(\lambda)$ and $R^{(\bar{3},\bar{3})}(\lambda)$ respectively. For a general discussion of R-matrices alternating between the vector representation of $U_q[sl(n|m)]$ and its dual see for instance [12–15]. In the specific case of the quantum superalgebra $U_q[sl(2|1)]$ the above set of R-matrices have been explicitly discussed in [8] for a particular grading (models of this type without grading have been introduced before by Perk and Schultz [16]). In what follows we shall present their expressions for arbitrary ordering of the Grassmann parities,

$$
\mathcal{R}_{a,b}^{(33)}(\lambda) = \sum_{j=1}^{3} a_j(\lambda) e_{j,j}^{(a)} \otimes e_{j,j}^{(b)} + b(\lambda) \sum_{\substack{j,k=1 \\ j \neq k}}^{3} e_{j,j}^{(a)} \otimes e_{k,k}^{(b)} + c(\lambda) \left\{ \sum_{\substack{j,k=1 \\ j>k}}^{3} (-1)^{p_j p_k} e_{j,k}^{(a)} \otimes e_{k,j}^{(b)} \right.
$$
$$
\left. + \exp(-2\lambda) \sum_{\substack{j,k=1 \\ j<k}}^{3} (-1)^{p_j p_k} e_{j,k}^{(a)} \otimes e_{k,j}^{(b)} \right\}, \tag{2.1}
$$

$$
\mathcal{R}_{a,b}^{(3\bar{3})}(\lambda) = \sum_{j=1}^{3} a_j(-\lambda - i\gamma) e_{j,j}^{(a)} \otimes e_{j,j}^{(b)} + b(-\lambda - i\gamma) \sum_{\substack{j,k=1 \\ j \neq k}}^{3} e_{j,j}^{(a)} \otimes e_{k,k}^{(b)}
$$
$$
+ c(-\lambda - i\gamma) \left\{ \sum_{\substack{j,k=1 \\ j<k}}^{3} (-1)^{p_j} q^{-2\delta_{j,1}} e_{j,k}^{(a)} \otimes e_{j,k}^{(b)} + \exp(2\lambda + 2i\gamma) \sum_{\substack{j,k=1 \\ j>k}}^{3} (-1)^{p_j} q^{2\delta_{k,1}} e_{j,k}^{(a)} \otimes e_{j,k}^{(b)} \right\}, \tag{2.2}
$$

$$
\mathcal{R}_{a,b}^{(\bar{3}3)}(\lambda) = \sum_{j=1}^{3} a_j(-\lambda) e_{j,j}^{(a)} \otimes e_{j,j}^{(b)} + b(-\lambda) \sum_{\substack{j,k=1 \\ j \neq k}}^{3} e_{j,j}^{(a)} \otimes e_{k,k}^{(b)} + c(-\lambda) \left\{ \sum_{\substack{j,k=1 \\ j>k}}^{3} (-1)^{p_k} f(k,j)^{-1} e_{j,k}^{(a)} \otimes e_{j,k}^{(b)} \right.
$$
$$
\left. + \exp(2\lambda) \sum_{\substack{j,k=1 \\ j<k}}^{3} (-1)^{p_k} f(j,k) e_{j,k}^{(a)} \otimes e_{j,k}^{(b)} \right\}, \tag{2.3}
$$

$$\mathcal{R}_{a,b}^{(\bar{3}\bar{3})}(\lambda) = \sum_{j=1}^{3} a_j(\lambda) e_{j,j}^{(a)} \otimes e_{j,j}^{(b)} + b(\lambda) \sum_{\substack{j,k=1 \\ j \neq k}}^{3} e_{j,j}^{(a)} \otimes e_{k,k}^{(b)} + c(\lambda) \left\{ \sum_{\substack{j,k=1 \\ j<k}}^{3} (-1)^{p_j p_k} e_{j,k}^{(a)} \otimes e_{k,j}^{(b)} \right.$$

$$\left. + \exp(-2\lambda) \sum_{\substack{j,k=1 \\ j>k}}^{3} (-1)^{p_j p_k} e_{j,k}^{(a)} \otimes e_{k,j}^{(b)} \right\}, \tag{2.4}$$

where $e_{j,k}^{(a)} \in \text{End}(\mathbb{C}_a^3)$ are the standard 3×3 Weyl matrices. The symbol p_j denote the Grassmann parities distinguishing the bosonic $p_j = 0$ and fermionic $p_j = 1$ degrees of freedom.

The dependence of the Boltzmann weights $a_j(\lambda)$, $b(\lambda)$ and $c(\lambda)$ on the spectral parameter are,

$$a_j(\lambda) = \frac{\sinh\left[\lambda - i(2p_j - 1)\gamma\right]}{\sinh\left[\lambda + i\gamma\right]}, \quad b(\lambda) = \frac{\sinh\left[\lambda\right]}{\sinh\left[\lambda + i\gamma\right]}, \quad c(\lambda) = \exp[\lambda] \frac{\sinh\left[i\gamma\right]}{\sinh\left[\lambda + i\gamma\right]}, \tag{2.5}$$

while functions $f(j,k)$ depend only on the anisotropy γ as follows,

$$f(1,2) = \exp[2i\gamma(1 - p_3)], \quad f(1,3) = \exp[2i\gamma p_2], \quad f(2,3) = \exp[-2i\gamma p_1]. \tag{2.6}$$

The R-matrices defined above fulfill the Yang-Baxter equation on any tensor product built up from the 3 and $\bar{3}$ representation, namely

$$R_{12}^{(\omega_1,\omega_2)}(\lambda) R_{13}^{(\omega_1,\omega_3)}(\lambda + \mu) R_{23}^{(\omega_2,\omega_3)}(\mu) = R_{23}^{(\omega_2,\omega_3)}(\mu) R_{13}^{(\omega_1,\omega_3)}(\lambda + \mu) R_{12}^{(\omega_1,\omega_2)}(\lambda), \tag{2.7}$$

where the representations $\omega_j \in \{3, \bar{3}\}$ for $j = 1, 2, 3$.

One consequence of these set of Yang-Baxter relations is that there exists two different types of Lax operators obeying the Yang-Baxter algebra with the same R-matrix. For example, this means that an integrable vertex model combining the $R^{(3,3)}(\lambda)$ and $R^{(3,\bar{3})}(\lambda)$ can be constructed within the framework of the quantum inverse scattering method. As usual the respective row-to-row transfer matrix is written as the supertrace [17] over the auxiliary space $\mathcal{A} \sim \mathbb{C}^3$ of the following ordered product of operators:

$$T^{(3)}(\lambda, \xi) = \text{Str}_{\mathcal{A}} \left[\mathcal{R}_{\mathcal{A}2L}^{(3,3)}(\lambda) \mathcal{R}_{\mathcal{A}2L-1}^{(3,\bar{3})}(\lambda - i\gamma + \xi) \mathcal{R}_{\mathcal{A}2L-2}^{(3,3)}(\lambda) \cdots \mathcal{R}_{\mathcal{A}1}^{(3,\bar{3})}(\lambda - i\gamma + \xi) \right] \tag{2.8}$$

acting on the Hilbert space $(3 \otimes \bar{3})^{\otimes L} \sim \mathbb{C}^{2L}$. The alternation on the spectral parameter can be introduced since the R-matrices are additive on λ. Note that this choice of inhomogeneity does not spoil the basic properties such as the symmetry and locality of the interactions of the corresponding alternating superspin chain with the Hamiltonian obtained by taking the logarithmic derivative of $T^{(3)}(\lambda, \xi)$ at $\lambda = 0$.

By the same token a solvable integrable vertex model alternating the R-matrices $R^{(\bar{3},3)}(\lambda)$ and $R^{(\bar{3},\bar{3})}(\lambda)$ can be constructed. The expression of the transfer matrix mixing such operators is

$$T^{(\bar{3})}(\lambda, \bar{\xi}) = \mathrm{Str}_{\mathcal{A}} \left[\mathcal{R}^{(\bar{3},3)}_{\mathcal{A}2L}(\lambda + i\gamma - \bar{\xi}) \mathcal{R}^{(\bar{3},\bar{3})}_{\mathcal{A}2L-1}(\lambda) \mathcal{R}^{(\bar{3},3)}_{\mathcal{A}2L-2}(\lambda + i\gamma - \bar{\xi}) \cdots \mathcal{R}^{(\bar{3},\bar{3})}_{\mathcal{A}1}(\lambda) \right]. \tag{2.9}$$

acting on the same Hilbert space as (2.8) above. Again, an alternating superspin chain can be constructed by expansion of the transfer matrix around $\lambda = 0$.

It turns out that – in addition to commuting among themselves – the transfer matrices $T^{(3)}(\lambda, \xi)$ and $T^{(\bar{3})}(\lambda, \bar{\xi})$ constitute a family of commuting operators when the inhomogeneities ξ and $\bar{\xi}$ are the same, i.e.

$$\left[T^{(3)}(\lambda, \xi), T^{(\bar{3})}(\mu, \xi) \right] = 0, \quad \forall \lambda, \mu. \tag{2.10}$$

The property (2.10) relies on the fact that we have chosen an identical ordering of representations 3 and $\bar{3}$ in the definition of the Hilbert spaces for the transfer matrices (2.8) and (2.9) and follows from the Yang-Baxter equation (2.7) once we choose the representations $\omega_1 = 3$, $\omega_2 = \bar{3}$ and $\omega_3 = 3, \bar{3}$. In this situation we are able to construct an integrable vertex model that alternates representations 3 and $\bar{3}$ both on horizontal *and* vertical spaces of states of a square lattice of size $2L \times 2L$. The respective 'double row' transfer matrix of such model is obtained by taking the following product,

$$T^{(mix)}(\lambda, \xi) = T^{(3)}(\lambda, \xi) T^{(\bar{3})}(\lambda, \xi). \tag{2.11}$$

By construction $T^{(mix)}(\lambda = 0, \xi)$ is proportional to the translation operator by two lattice sites. Therefore, we can define an integrable superspin Hamiltonian,

$$\mathcal{H}^{(mix)} = i \left. \frac{\partial}{\partial \lambda} \ln T^{(mix)}(\lambda, \xi) \right|_{\lambda=0}. \tag{2.12}$$

The expression for $H^{(mix)}$ in terms of the R-matrices can be obtained by computing the individual Hamiltonians associated with the transfer matrices $T^{(3)}(\lambda)$ and $T^{(\bar{3})}(\lambda)$. The technicalities entering this computation are cumbersome but the final result is somehow simple,

$$\mathcal{H}^{(mix)} = i \sum_{\substack{j=2 \\ \mathrm{mod}\,2}}^{2L} \left[\mathcal{R}^{(3,\bar{3})}_{j,j+1}(\xi - i\gamma) \right]^{-1} \left[\dot{\mathcal{R}}^{(3,\bar{3})}_{j,j+1}(\xi - i\gamma) + P_{j,j+2} \dot{\mathcal{R}}^{(3,3)}_{j,j+2}(0) \mathcal{R}^{(3,\bar{3})}_{j,j+1}(\xi - i\gamma) \right]$$

$$+ i \sum_{\substack{j=1 \\ \mathrm{mod}\,2}}^{2L} \left[\mathcal{R}^{(\bar{3},3)}_{j,j+1}(i\gamma - \xi) \right]^{-1} \left[\dot{\mathcal{R}}^{(\bar{3},3)}_{j,j+1}(i\gamma - \xi) + P_{j,j+2} \dot{\mathcal{R}}^{(\bar{3},\bar{3})}_{j,j+2}(0) \mathcal{R}^{(\bar{3},3)}_{j,j+1}(i\gamma - \xi) \right] \tag{2.13}$$

where periodic boundary conditions $2L + 1 \equiv 1$ and $2L + 2 \equiv 2$ are assumed. The operator P_{ab} is the graded permutation $P_{ab} = \sum_{j,k=1}^{3} (-1)^{p_j p_k} e_{j,k}^{(a)} \otimes e_{k,j}^{(b)}$ and $\dot{\mathcal{R}}_{ab}(\lambda)$ denotes the derivative of the R-matrix $\mathcal{R}_{ab}(\lambda)$ with respect to the spectral parameter λ.

The diagonalization of the above transfer matrix can be carried out by applying the nested algebraic Bethe ansatz approach [18, 19]. For this particular mixed vertex model the essential tools to obtain the eigenvalues of $T^{(mix)}(\lambda, \xi)$ can for instance be found in [20]. We shall not repeat here these technical details and concentrate our attention only to the main results. As usual the expressions for the eigenvalues obtained in this approach will depend on the choice of grading [17, 21–24]. For later convenience we use $[p_1, p_2, p_3] = [0, 1, 0]$ in the following. Let $\Lambda_{N_1, N_2}^{(mix)}(\lambda)$ denote the eigenvalues of $T^{(mix)}(\lambda, \xi)$ in the sector of the Hilbert space selected by fixing the two conserved quantum numbers related to the $U(1)$ subalgebras of $U_q[sl(2|1)$, i.e. charge $b = (N_1 - N_2)/2$ and z-component of the spin $s_3 = L - (N_1 + N_2)/2$. As a consequence of (2.10) the eigenvalues can be factorized

$$\Lambda_{N_1, N_2}^{(mix)}(\lambda) = \Lambda_{N_1, N_2}^{(3)}(\lambda) \Lambda_{N_1, N_2}^{(\bar{3})}(\lambda). \tag{2.14}$$

Here $\Lambda_{N_1, N_2}^{(3)}(\lambda)$ and $\Lambda_{N_1, N_2}^{(\bar{3})}(\lambda)$ are the corresponding eigenvalues associated to the transfer matrices $T^{(3)}(\lambda, \xi)$ and $T^{(\bar{3})}(\lambda, \xi)$ respectively.

It turns out that the expressions for the eigenvalues $\Lambda_{N_1, N_2}^{(3)}(\lambda)$ and $\Lambda_{N_1, N_2}^{(\bar{3})})(\lambda)$ are given by,

$$
\Lambda_{N_1, N_2}^{(3)}(\lambda) = \left[\frac{\sinh(\lambda + \xi)}{\sinh(\lambda + \xi - i\gamma)} \right]^L \prod_{j=1}^{N_1} \frac{\sinh(\lambda_j^{(1)} - \lambda + i\gamma/2)}{\sinh(\lambda_j^{(1)} - \lambda - i\gamma/2)} + \left[\frac{\sinh(\lambda)}{\sinh(\lambda + i\gamma)} \right]^L \prod_{j=1}^{N_2} \frac{\sinh(\lambda - \lambda_j^{(2)} + i\gamma)}{\sinh(\lambda - \lambda_j^{(2)})}
$$
$$
- \left[\frac{\sinh(\lambda + \xi)\sinh(\lambda)}{\sinh(\lambda + i\gamma)\sinh(\lambda + \xi - i\gamma)} \right]^L \prod_{j=1}^{N_1} \frac{\sinh(\lambda - \lambda_j^{(1)} - i\gamma/2)}{\sinh(\lambda - \lambda_j^{(1)} + i\gamma/2)} \prod_{j=1}^{N_2} \frac{\sinh(\lambda_j^{(2)} - \lambda - i\gamma)}{\sinh(\lambda_j^{(2)} - \lambda)},
$$
$$\tag{2.15}$$

and

$$
\Lambda_{N_1, N_2}^{(\bar{3})}(\lambda) = \left[\frac{\sinh(\lambda)}{\sinh(\lambda + i\gamma)} \right]^L \prod_{j=1}^{N_1} \frac{\sinh(\lambda - \lambda_j^{(1)} - \xi + 3i\gamma/2)}{\sinh(\lambda - \lambda_j^{(1)} - \xi + i\gamma/2)}
$$
$$
+ \left[\frac{\sinh(\lambda - \xi + i\gamma)}{\sinh(\lambda - \xi)} \right]^L \prod_{j=1}^{N_2} \frac{\sinh(\lambda_j^{(2)} - \lambda + \xi)}{\sinh(\lambda_j^{(2)} - \lambda + \xi - i\gamma)}
$$
$$
- \left[\frac{\sinh(\lambda - \xi + i\gamma)\sinh(\lambda)}{\sinh(\lambda + i\gamma)\sinh(\lambda - \xi)} \right]^L \prod_{j=1}^{N_1} \frac{\sinh(\lambda_j^{(1)} - \lambda + \xi - 3i\gamma/2)}{\sinh(\lambda_j^{(1)} - \lambda + \xi - i\gamma/2)} \prod_{j=1}^{N_2} \frac{\sinh(\lambda - \lambda_j^{(2)} - \xi)}{\sinh(\lambda - \lambda_j^{(2)} - \xi + i\gamma)},
$$
$$\tag{2.16}$$

where the rapidities $\lambda_j^{(1)}$ and $\lambda_j^{(2)}$ satisfy the following set of nested Bethe equations,

$$
\left[\frac{\sinh(\lambda_j^{(1)} + i\gamma/2)}{\sinh(\lambda_j^{(1)} - i\gamma/2)}\right]^L = \prod_{k=1}^{N_2} \frac{\sinh(\lambda_j^{(1)} - \lambda_k^{(2)} + i\gamma/2)}{\sinh(\lambda_j^{(1)} - \lambda_k^{(2)} - i\gamma/2)}, \quad j = 1, \cdots, N_1,
$$

$$
\left[\frac{\sinh(\lambda_j^{(2)} + \xi)}{\sinh(\lambda_j^{(2)} + \xi - i\gamma)}\right]^L = \prod_{k=1}^{N_1} \frac{\sinh(\lambda_j^{(2)} - \lambda_k^{(1)} + i\gamma/2)}{\sinh(\lambda_j^{(2)} - \lambda_k^{(1)} - i\gamma/2)}, \quad j = 1, \cdots, N_2.
$$

(2.17)

Note that for the particular choice $\xi = i\gamma/2$ these Bethe ansatz equations become symmetrical on the variables $\lambda_j^{(1)}$ and $\lambda_j^{(2)}$. In the following we will concentrate our studies on this case. The eigenvalues of the Hamiltonian (2.12) corresponding to a solution of (2.17) are

$$
\begin{aligned}
E_{N_1,N_2}^{(mix)}(\gamma) &= i \left. \frac{\partial}{\partial\lambda} \ln \Lambda_{N_1,N_2}^{(mix)}(\lambda, i\gamma/2) \right|_{\lambda=0} \\
&= 4L \cot \frac{\gamma}{2} + 2 \left(\sum_{k=1}^{N_1} \frac{\sin\gamma}{\cos\gamma - \cosh 2\lambda_k^{(1)}} + \sum_{k=1}^{N_2} \frac{\sin\gamma}{\cos\gamma - \cosh 2\lambda_k^{(2)}} \right).
\end{aligned}
$$

(2.18)

Considering the above solution one sees that the spectrum at the points γ and $2\pi - \gamma$ are related to each other by only a sign,

$$
E_{N_1,N_2}^{(mix)}(\gamma) = -E_{N_1,N_2}^{(mix)}(2\pi - \gamma).
$$

(2.19)

III.   THE TWISTED XXZ SPIN-1 MODEL

The classical vertex model associated to the integrable Heisenberg XXZ spin-1 chain turns out to be the three-state factorized R-matrix found by Zamolodchikov and Fateev [9]. Considering our previous notation this operator can be expressed as

$$
\begin{aligned}
\mathcal{R}_{ab}(\lambda) =\ & e_{1,1}^{(a)} \otimes e_{1,1}^{(a)} + e_{3,3}^{(a)} \otimes e_{3,3}^{(b)} + \bar{f}(\lambda) \left[e_{1,1}^{(a)} \otimes e_{3,3}^{(b)} + e_{3,3}^{(a)} \otimes e_{1,1}^{(b)} \right], \\
&+ \bar{b}(\lambda) \left[e_{1,1}^{(a)} \otimes e_{2,2}^{(b)} + e_{2,2}^{(a)} \otimes e_{1,1}^{(b)} + e_{2,2}^{(a)} \otimes e_{3,3}^{(b)} + e_{3,3}^{(a)} \otimes e_{2,2}^{(b)} + e_{2,2}^{(a)} \otimes e_{2,2}^{(b)} \right] \\
&+ \bar{c}(\lambda) \left[e_{1,2}^{(a)} \otimes e_{2,1}^{(b)} + e_{2,1}^{(a)} \otimes e_{1,2}^{(b)} + e_{2,3}^{(a)} \otimes e_{3,2}^{(b)} + e_{3,2}^{(a)} \otimes e_{2,3}^{(b)} \right] \\
&+ \bar{d}(\lambda) \left[e_{1,2}^{(a)} \otimes e_{3,2}^{(b)} + e_{2,3}^{(a)} \otimes e_{2,1}^{(b)} + e_{2,1}^{(a)} \otimes e_{2,3}^{(b)} + e_{3,2}^{(a)} \otimes e_{1,2}^{(b)} \right] \\
&+ \bar{h}(\lambda) \left[e_{1,3}^{(a)} \otimes e_{3,1}^{(b)} + e_{2,2}^{(a)} \otimes e_{2,2}^{(b)} + e_{3,1}^{(a)} \otimes e_{1,3}^{(b)} \right]
\end{aligned}
$$

(3.1)

where the corresponding Boltzmann weights $\bar{b}(\lambda)$, $\bar{c}(\lambda)$, $\bar{d}(\lambda)$, $\bar{f}(\lambda)$ and $\bar{h}(\lambda)$ are given by,

$$
\bar{b}(\lambda) = \frac{\sinh(\lambda)}{\sinh(\lambda + i\gamma)}, \quad \bar{c}(\lambda) = \frac{\sinh(i\gamma)}{\sinh(\lambda + i\gamma)}, \quad \bar{d}(\lambda) = \frac{\sinh(i\gamma)\sinh(\lambda)}{\sinh(\lambda + i\frac{\gamma}{2})\sinh(\lambda + i\gamma)},
$$

$$
\bar{f}(\lambda) = \frac{\sinh(\lambda - i\frac{\gamma}{2})\sinh(\lambda)}{\sinh(\lambda + i\frac{\gamma}{2})\sinh(\lambda + i\gamma)}, \quad \bar{h}(\lambda) = \frac{2\cosh(\frac{i\gamma}{2})\left[\sinh(i\frac{\gamma}{2})\right]^2}{\sinh(\lambda + i\frac{\gamma}{2})\sinh(\lambda + i\gamma)}.
$$

(3.2)

With (3.1) the respective transfer-matrix $T(\lambda)$ with toroidal boundary conditions can formally be constructed as follows

$$T(\lambda) = Tr_{\mathcal{A}}\left[G_{\mathcal{A}}\mathcal{R}_{\mathcal{A}L}(\lambda)\mathcal{R}_{\mathcal{A}L-1}(\lambda)\cdots\mathcal{R}_{\mathcal{A}1}(\lambda)\right], \tag{3.3}$$

where $G_{\mathcal{A}}$ denotes a 3×3 matrix representing the twisted boundary condition.

The diagonal twisted boundary condition compatible with integrability is obtained by choosing the matrix G as,

$$G_{\mathcal{A}} = \begin{pmatrix} 1 & 0 & 0 \\ 0 & \mathrm{e}^{i\varphi} & 0 \\ 0 & 0 & \mathrm{e}^{2i\varphi} \end{pmatrix}, \tag{3.4}$$

where the angle φ is assumed to be in the interval $0 \leq \varphi \leq \pi$.

The transfer matrix (3.3) with (3.4) can be diagonalized with very little difference from the periodic case since the presence of the diagonal boundary matrix $G_{\mathcal{A}}$ preserves the $U(1)$ bulk symmetry. The respective eigenvalues can be determined either by using the mechanism of fusion [25–27] or by applying the algebraic Bethe ansatz construction developed in [28]. As a consequence of the $U(1)$ invariance of the transfer matrix the Hilbert space can be separated in disjoint sectors corresponding to total magnetization s_3. Starting from the state with maximal $s_3 = L$ one obtains the following expression of the corresponding eigenvalues $\Lambda_N(\lambda, \varphi)$ in the sector $s_3 = L - N$, $N = 0, \cdots, L$

$$\Lambda_N(\lambda, \varphi) = \prod_{j=1}^{N} \frac{\sinh(\lambda_j - \lambda + i\gamma/2)}{\sinh(\lambda_j - \lambda - i\gamma/2)} + \mathrm{e}^{2i\varphi}\left[\frac{\sinh(\lambda - i\gamma/2)\sinh(\lambda)}{\sinh(\lambda + i\gamma)\sinh(\lambda + i\gamma/2)}\right]^L \prod_{j=1}^{N} \frac{\sinh(\lambda - \lambda_j + i\gamma)}{\sinh(\lambda - \lambda_j)}$$

$$+ \mathrm{e}^{i\varphi}\left[\frac{\sinh(\lambda)}{\sinh(\lambda + i\gamma)}\right]^L \prod_{j=1}^{N} \frac{\sinh(\lambda - \lambda_j + i\gamma)\sinh(\lambda - \lambda_j - i\gamma/2)}{\sinh(\lambda - \lambda_j + i\gamma/2)\sinh(\lambda - \lambda_j)}, \tag{3.5}$$

where the rapidities λ_j satisfy the following Bethe ansatz equations,

$$\left[\frac{\sinh(\lambda_j + i\gamma/2)}{\sinh(\lambda_j - i\gamma/2)}\right]^L = \mathrm{e}^{i\varphi}\prod_{\substack{k=1\\k\neq j}}^{N} \frac{\sinh(\lambda_j - \lambda_k + i\gamma/2)}{\sinh(\lambda_j - \lambda_k - i\gamma/2)}, \quad j = 1, \cdots, N. \tag{3.6}$$

At this point we have gathered the basic ingredients allowing to establish a mapping among part of the spectrum of the mixed transfer matrix (2.11) and the eigenvalues of the XXZ spin-1 model with special toroidal boundary condition for the special choice of $\xi = i\gamma/2$ in the transfer matrix $T^{(mix)}(\lambda)$ of the mixed spin chain: as mentioned above the Bethe ansatz equations (2.17) become symmetric between the two levels for this choice of ξ and their structure resembles that of

the Bethe ansatz equations (3.6) of the $XXZ-1$ chain with twist $\varphi = \pi$. In particular we find that in the sector $N_1 = N_2 = N$ of the Hilbert space of the mixed chain (this is where the total $U_q[sl(2|1)]$ charge b of the Bethe state is zero) there exists a subset of eigenstates parametrized by Bethe roots which can be identified with eigenstates of the spin-1 chain in the sector $s_3 = L - N$ by setting $\lambda_j^{(1)} = \lambda_j^{(2)} \equiv \lambda_j$. A similar correspondence has been observed between a subset of eigenvalues of the alternating $sl(2|1)$ superspin chain obtained in the limit $\gamma \to 0$ from the mixed chain considered here and the $SU(2)$-invariant spin-1 Takhtajan-Babujian chain [4]. For such states, a direct inspection of the expressions for the eigenvalues (2.15), (2.16), (3.5) leads us to the following relation,

$$\Lambda_{N,N}^{(mix)}(\lambda) = \left[\frac{\sinh(\lambda + i\gamma/2)}{\sinh(\lambda - i\gamma/2)}\right]^{2L} [\Lambda_N(\lambda, \varphi = \pi)]^2. \tag{3.7}$$

As a consequence, we obtain from (2.18) a relation between the energy eigenvalues of the XXZ spin-1 chain with L sites and those of the $U_q[sl(2|1)]$ superspin chain with $2L$ sites of alternating representations 3 and $\bar{3}$:

$$E_{N,N}^{(mix)} = 4L \cot(\gamma/2) + 2E_N^{(XXZ)}(\varphi = \pi) \tag{3.8}$$

where

$$E_N^{(XXZ)}(\varphi) = i \left.\frac{\partial}{\partial\lambda} \ln \Lambda_n(\lambda, \varphi)\right|_{\lambda=0} = \sum_{k=1}^{N} \frac{\sin\gamma}{\cos\gamma - \cosh 2\lambda_k} \tag{3.9}$$

is the energy eigenvalue of the XXZ spin-1 chain corresponding to a solution of the Bethe equations (3.6). As in Eq. (2.19) for the mixed superspin chain the spectrum of the XXZ model is inverted at anisotropy $\gamma = \pi$, i.e. $\mathrm{spec}(\gamma) \leftrightarrow -\mathrm{spec}(2\pi - \gamma)$.

In the thermodynamic limit $L \to \infty$ the solutions of the Bethe equations (3.6) are grouped into 'strings' consisting of m complex rapidities $\lambda_j^{(m)}$ characterized by a common real center $\lambda^{(m)}$ and a parity $v_m = \pm 1$:

$$\lambda_j^{(m)} = \lambda^{(m)} + i\frac{\gamma}{4}(m + 1 - 2j) + i\frac{\pi}{4}(1 - v_m), \quad j = 1, \ldots, m. \tag{3.10}$$

The allowed values of (m, v_m) depend on the anisotropy γ in an involved way [26, 29]. Here we shall not go into the details of the string classification: for the range of anisotropies $0 \leq \gamma < \pi$ that we are considering in this paper it is found that the most relevant root configurations solving (3.6) can be organized into strings $(1, +)$, $(1, -)$ and $(2, +)$.

A.   The disordered antiferromagnet regime of the spin-1 chain

Most importantly, the ground state of the system without twist, $\varphi = 0$, and on an even length lattice is a condensate of $L/2$ $(2, +)$-strings in this regime [25, 26, 30]. In the thermodynamic limit one can compute the energy per site giving $\epsilon_\infty(\gamma) = -2 \cot(\gamma/2)$. The finite size spectrum of the XXZ spin-1 model without twist has been investigated in [31, 32]: in the entire interval $0 \leq \gamma < \pi$ the spectrum has gapless excitations with Fermi velocity $v_F = 2\pi/\gamma$. The central charge of the conformal field theory describing the low energy sector is $c = 3/2$, hence the ground state energy for even L scales as

$$E^{(XXZ)}(\varphi = 0) - L\epsilon_\infty(\gamma) = -\frac{\pi v_F}{6L} c + o(\frac{1}{L}) = -\frac{\pi v_F}{4L} + o(\frac{1}{L}). \qquad (3.11)$$

The operators of this CFT are given by products of Ising operators and $U(1)$ Kac-Moody fields. The scaling dimensions of these composite fields in the presence of a twist φ are [33]

$$X_{(r,j)}^{(n,m+\varphi/\pi)}(\gamma) = X_I(r,j) + n^2 X_c + \left(m + \frac{\varphi}{\pi}\right)^2 \frac{1}{16 X_c}, \quad X_c = \frac{\pi - \gamma}{4\pi},$$

$$X_I(0,0) \in \{0, 1\}, \quad X_I(0,1) = X_I(1,0) = \frac{1}{8}, \quad X_I(1,1) = \frac{1}{2}. \qquad (3.12)$$

Depending on the parity of L the possible subset of the KM representations is determined by the selection rules

$$n = r + L \mod 2, \quad m = j + L \mod 2 \qquad (3.13)$$

for given parity j and toroidal b.c. (type r) of the Ising sector. The smallest exponents obtained from (3.12) for even L are

$$X_{(0,0)}^{(0,0+\varphi/\pi)}(\gamma) = \left(\frac{\varphi}{\pi}\right)^2 \frac{1}{16 X_c},$$

$$X_{(0,1)}^{(0,-1+\varphi/\pi)}(\gamma) = \frac{1}{8} + \left(1 - \frac{\varphi}{\pi}\right)^2 \frac{1}{16 X_c}, \qquad (3.14)$$

$$X_{(1,0)}^{(1,0+\varphi/\pi)}(\gamma) = \frac{1}{8} + X_c + \left(\frac{\varphi}{\pi}\right)^2 \frac{1}{16 X_c},$$

and for L odd

$$X_{(1,0)}^{(0,-1+\varphi/\pi)}(\gamma) = \frac{1}{8} + \left(1 - \frac{\varphi}{\pi}\right)^2 \frac{1}{16 X_c},$$

$$X_{(0,0)}^{(1,-1+\varphi/\pi)}(\gamma) = X_c + \left(1 - \frac{\varphi}{\pi}\right)^2 \frac{1}{16 X_c}, \qquad (3.15)$$

$$X_{(0,1)}^{(1,0+\varphi/\pi)}(\gamma) = \frac{1}{8} + X_c + \left(\frac{\varphi}{\pi}\right)^2 \frac{1}{16 X_c}.$$

As the twist is varied the energy of the $\varphi = 0$ ground state $((r,j) = (0,0), (m,n) = (0,0)$ for even L) increases until there occurs a crossing with the level evolving from $(n, m) = (0, -1)$ at
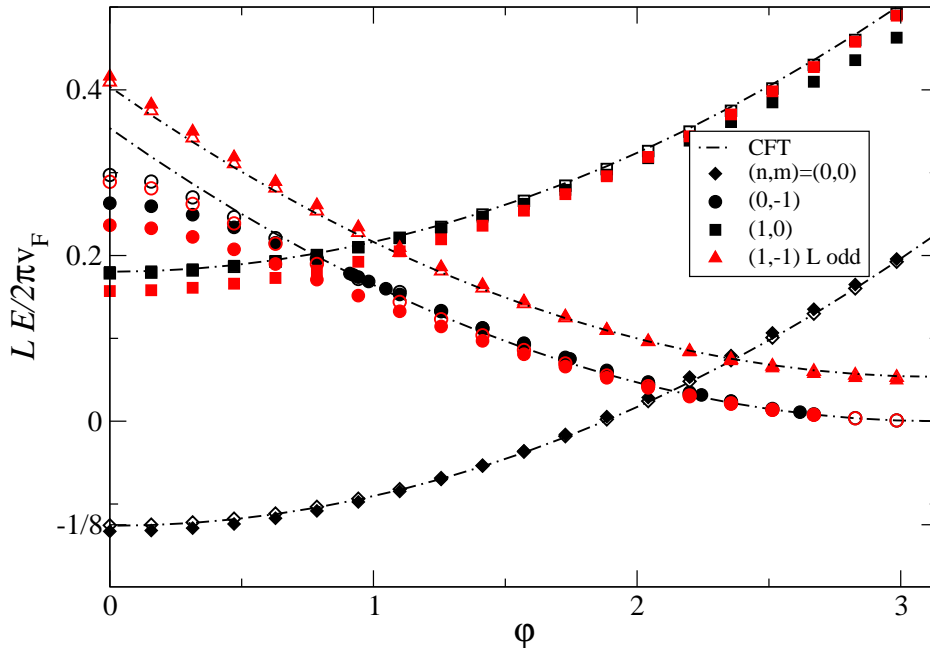
FIG. 1. Evolution of the ground state and lowest excitation energies of the XXZ spin-1 model with $\gamma = \frac{2\pi}{7}$ as a function of twist φ. Filled (open) symbols in black are for $L = 6$ (30), respectively; red symbols for $L = 7$ (31). Dash-dotted lines indicate the CFT predictions (3.12).

$\varphi = (3\pi - \gamma)/4$ (see Fig. 1). The conformal dimension of this state at twist $\varphi = \pi$ is $X_{0,1}^{0,0} = 1/8$ for even and $X_{1,0}^{0,0} = 1/8$ for odd length lattices independent of the deformation parameter γ. Together with the finite size scaling of the ground state energy (3.11) this gives a state whose energy is $L\epsilon_\infty(\gamma)$ *without any finite size corrections*! Note that the corresponding wave function does vary with γ. According to (3.9) this can only be realized with a highly degenerate configuration of Bethe roots, namely $\lambda_k \equiv 0$ for all $k = 1, \ldots, L$. The identification (3.8) implies the existence of a zero energy eigenstate of the mixed $U_q[sl(2|1)]$ superspin model in the singlet sector of the latter. For $0 \leq \gamma \leq \pi/2$ this is the ground state of the π-twisted XXZ spin-1 chain and the mixed superspin chain, implying that the effective central charges of this models are $c = 0$. For $\gamma > \pi/2$, the two-fold degenerate level with scaling dimension $X_{0,0}^{1,-1+\varphi/\pi}$ realized in the XXZ spin-1 chain of odd length has a lower energy at twist $\varphi = \pi$. The consequences of this crossing for the superspin chain will be discussed below.

B.   The disordered ferromagnetic regime of the spin-1 chain

As a consequence of the inversion of the spectrum under $\gamma \leftrightarrow \tilde{\gamma} \equiv 2\pi - \gamma$ we can discuss the properties of the spin-1 chain in this regime in the same interval $0 < \gamma < \pi$ while changing the

sign of the energies (3.9). This leaves the string classification (3.10) unchanged. Without twist in the boundary conditions the configuration of Bethe roots corresponding to the ground state in the disordered ferromagnetic regime is given by a filled sea of L $(1,-)$-strings. Above this state there are gapless low energy excitations with Fermi velocity $\tilde{v}_F = 2\pi/(2\pi - \gamma)$. The corresponding conformal field theory has been identified as a $U(1)$ Gaussian model with central charge $c = 1$ and scaling dimensions of the primary operators given by [34]

$$\tilde{X}_{n,m}(\gamma) = n^2 x_p + \frac{m^2}{4x_p}, \qquad x_p = \frac{\gamma}{4\pi} \tag{3.16}$$

where n and m take integer values which determine the magnetization $s_3 = n$ and vorticity of the corresponding state. Note that the compactification radius of the boson $R = \sqrt{x_p}$ vanishes as $\gamma \to 0$ indicating the transition into the non-conformal isotropic ferromagnetic state. For toroidal boundary conditions with twist φ one has to replace $m \to m + \varphi/2\pi$ in Eq. (3.16). The adiabatic evolution of the Bethe roots under the twist is rather involved, a detailed study of the corresponding regime in the spin-1/2 XXZ chain can be found in Ref. 35.

Here our focus is on the antiperiodic twisted chain: choosing $\varphi = \pi$ implies that the finite size gaps are given by Eq. (3.16) with integer n but half-odd integer $m = \pm 1/2, \pm 3/2, \ldots$. As an immediate consequence the lowest state of the conformal part of the spectrum in the finite system has an energy ($\tilde{\epsilon}_\infty^{(XXZ)}$ is the bulk ground state energy density of the chain in this regime)

$$E_0(L) - L\tilde{\epsilon}_\infty^{(XXZ)} \simeq -\frac{\pi \tilde{v}_F}{6L} + \frac{2\pi \tilde{v}_F}{L} \tilde{X}_{0,\frac{1}{2}} = -\frac{\pi \tilde{v}_F}{6L} + \frac{2\pi \tilde{v}_F}{L} \frac{\pi}{4\gamma} \tag{3.17}$$

which grows as $\gamma \to 0$, eventually leaving the range of applicability of the finite size analysis based on Eq. (3.16).

For additional insights into the properties of the spin-1 chain we have to rely on the analysis of the Bethe equations (3.6): the configuration of Bethe roots for this state evolves as γ decreases from π to 0: for $\gamma \in (\pi/(k+1), \pi/k)$ we find that it consists of $L - k$ $(1,-)$-strings and a single $(k,+)$-string according to the classification (3.10), see Fig. 2. In the finite system the configuration reduces to a single $(L,+)$-string for $\gamma < \pi/L$. This is a bound state of magnon-excitations over the ferromagnetic pseudo vacuum state with $s_3 = L$. Based on this observation we propose that for a system of finite size L there is a level crossing at $\gamma = \pi/L$ leading to a fully polarized ground state at smaller values of the anisotropy. This proposal has been confirmed by numerical diagonalization of the Hamiltonian.
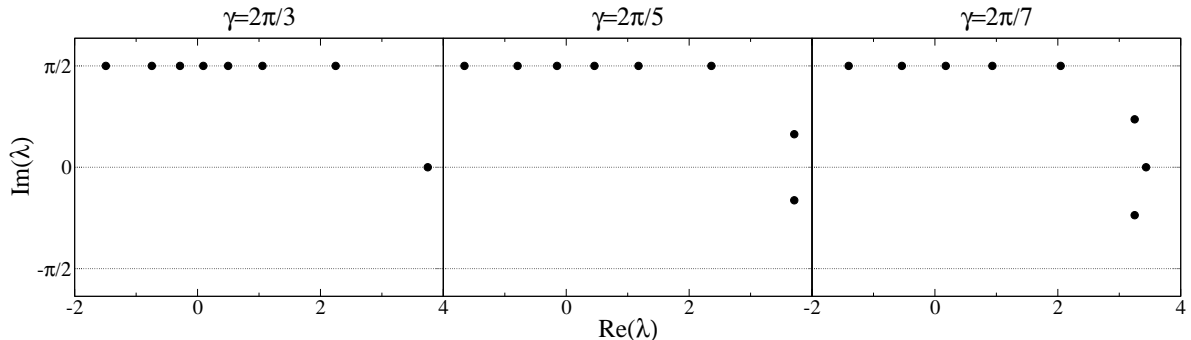
FIG. 2. Configuration of Bethe roots for the lowest $S_3 = 0$ state in the ferromagnetic disordered regime of the XXZ spin-1 chain with $L = 8$ sites for various values of γ.

IV.   ANTIFERROMAGNETIC REGIME OF THE MIXED CHAIN

To discuss the properties of the mixed superspin chain we also need to distinguish two cases:

$0 \leq \gamma < \pi$: in analogy to the XXZ spin-1 chain we will call this regime 'antiferromagnetic',

$\pi < \gamma \leq 2\pi$: this 'ferromagnetic' regime will be discussed in the next section.

The solutions to the Bethe equations for the mixed superspin chain (2.17) can be classified into strings – similarly as for the XXZ spin-1 chain in (3.10): in the large L limit Bethe roots with $Im(\lambda_j^{(\alpha)}) \neq 0$ or $\pi/2$ have to be combined such that their differences coincide with poles or zeroes of the bare scattering phase shifts on the right hand sides of Eqs. (2.17). As in the rational case of the $sl(2|1)$ mixed superspin chain [4] this considerations lead to

(1) 1-strings

just as for the XXZ spin-1 chain there are two types of unpaired roots allowed, namely real ones and roots on the line $Im(\lambda) = \pi/2$,

and to composites combining roots from both levels:

(2) wide and strange strings

these configurations consist of m roots from both levels of the Bethe ansatz with the same center $\lambda_m \in \mathbb{R} \cup (\mathbb{R} + i\pi/2)$. For m odd they have been called wide strings in Ref. 4, e.g.

$$\begin{aligned}
\lambda_{m,k}^{(1)} &= \lambda_m + i\frac{\gamma}{4}(m+3-4k), & k &= 1, \ldots, \frac{m+1}{2}, \\
\lambda_{m,j}^{(2)} &= \lambda_m + i\frac{\gamma}{4}(m+1-4j), & j &= 1, \ldots, \frac{m-1}{2}
\end{aligned} \tag{4.1}$$

and a second type obtained by interchanging first and second level roots, $\{\lambda_{m,k}^{(1)}\} \leftrightarrow \{\lambda_{m,j}^{(2)}\}$. For m even, the so-called strange strings have the unusual property of not being invariant under complex conjugation, e.g.

$$
\begin{aligned}
\lambda_{m,k}^{(1)} &= \lambda_m + i\frac{\gamma}{4}\left(m + 3 - 4k\right), \qquad k = 1, \ldots, \frac{m}{2}\,, \\
\lambda_{m,j}^{(2)} &= \lambda_m + i\frac{\gamma}{4}\left(m + 1 - 4j\right), \qquad j = 1, \ldots, \frac{m}{2}\,.
\end{aligned}
\tag{4.2}
$$

Again, there is a second type of such configurations for given m obtained by $\{\lambda_{m,k}^{(1)}\} \leftrightarrow \{\lambda_{m,j}^{(2)}\}$.

(3) narrow strings

Finally, there are composites which contain the same number $m/2$ of roots on either level. They may be seen as degenerations of two wide or strange strings with the same center λ_m.

The existence of strings of a given length as well as their parity (i.e. whether they are centered around the real axis or the line $Im(\lambda_m) = \pi/2$) depends on the deformation parameter γ, again as in the XXZ spin-1 chain. For the states with lowest (and highest) energies, we find that 1-strings of either parity and strange 2-strings centered around the real axis plus their possible degenerations into narrow ones are sufficient to capture the spectrum (in the 'ferromagnetic' high energy regime this is true at least for $\gamma > \pi/3$ as discussed in Section V below).

In the antiferromagnetic regime this classification is particularly useful in the sector where the total number of roots on the two levels is the same, i.e. for $N_1 = N_2$ in (2.17): here the total $U_q[sl(2|1)]$ charge of the Bethe state is zero. Many low lying excited states in this sector correspond to root configurations consisting of strange 2-strings (up to finite size corrections), i.e. sets $\{\lambda_k^{(1)}\}$ and $\{\lambda_k^{(2)}\}$ that are mapped onto each other by complex conjugation. This sector also contains the lowest state in the singlet sector of the model, where $N_1 = N_2 = L$. As has been argued above, this state is also present in spectrum of the XXZ spin-1 chain related by (3.8) and has energy $E^{(mix)} \equiv 0$. This is the ground state of the superspin chain for $\gamma < \pi/2$. The corresponding root configuration solving the Bethe equations (2.17) is $\lambda_k^{(a)} \equiv 0$ for *all* $k = 1, \ldots, L$ and $a = 1, 2$. The same observation has been made in the rational model obtained as $\gamma \to 0$ [4].

A. Small systems

For L up to 4 we have computed the complete spectrum of the mixed chain by exact numerical diagonalization of the Hamiltonian. As a consequence of the deformation some of the degenerations present in the $sl(2|1)$-symmetric superspin chain are lifted. For example, an $sl(2|1)$ octet $[b, s] =$

TABLE I. Low energy states of the $L = 3$ superspin chain in the antiferromagnetic regime for $\gamma = 2\pi/7$ and the identified Bethe configurations. Additional root configurations to these energies can be obtained by using the symmetries of the Bethe equations.

(N_1, N_2)	Energy E	degeneracy	Bethe roots
$(3,3)$	0	1	$\Lambda^{(1)} = \{0,0,0\} = \Lambda^{(2)}$ (XXZ)
$(2,2)$	1.2968	2	$\Lambda^{(1)} = \{\pm i0.2386\} = \Lambda^{(2)}$ (XXZ)
$(3,3)$	1.6523	2	$\Lambda^{(1)} = \{-0.0110 \pm i0.2348, \infty\} = -\Lambda^{(2)}$
$(3,2)$	2.3027	4	$\Lambda^{(1)} = \{\pm i0.2492, i\pi/2\}, \Lambda^{(2)} = \{\pm i0.2255\}$
$(2,2)$	4.9748	4	$\Lambda^{(1)} = \{\pm 0.1161 + i0.2704\} = (\Lambda^{(2)})^*$
$(3,3)$	$5.1859 \pm i0.6690$	2*2	$\Lambda^{(1)} = \{-0.1429 - i0.2668, 0.0932 - i0.2675, \infty\} = -\Lambda^{(2)}$
$(3,2)$	$6.1084 \pm i0.3325$	2*8	$\Lambda^{(1)} = \{-0.0889 + i0.2822, 0.1199 + i0.3044, 0.2581 - i0.8296\}$
			$\Lambda^{(2)} = \{-0.0790 - i0.2295, 0.1415 - i0.2039\}$

$[0,1]$ splits into two charge 0 doublets with $s_3 = \pm 1$ and $s_3 = 0$ respectively and a quartet with charge $\pm\frac{1}{2}$ and $s_3 = \pm\frac{1}{2}$:

$$
[0,1] \to \{|b=0, s_3=1\rangle, |b=0, s_3=-1\rangle\} \cup \{|b=0, s_3=0\rangle, |b=0, s_3=0\rangle\}
$$
$$
\cup \{|b=\frac{1}{2}, s_3=\frac{1}{2}\rangle, |b=\frac{1}{2}, s_3=-\frac{1}{2}\rangle, |b=-\frac{1}{2}, s_3=\frac{1}{2}\rangle, |b=-\frac{1}{2}, s_3=-\frac{1}{2}\rangle\}. \tag{4.3}
$$

Interestingly, we observe cases where pairs of the $s_3 = 0$ doublets arising from degenerate octets in the isotropic case split further into pairs with complex conjugate eigenvalues.

For $L = 3$ we have identified the low energy states in terms of their corresponding configuration of Bethe roots, see Table I for the spectrum at anisotropy $\gamma = 2\pi/7$ (the degeneracies found in the numerical solution can be reproduced by applying symmetry operations on the set of Bethe roots, i.e. $\Lambda^{(1)} \leftrightarrow \Lambda^{(2)}$ or $\Lambda^{(a)} \leftrightarrow -\Lambda^{(a)}$ for both $a = 1, 2$, and by using the global symmetries of the mixed chain, i.e. reversal of all spins). Although they are strongly deformed in some cases, the string content of these configurations according to the classification given above can be identified.

Based on the numerical and analytical data the following general picture for the lowest excitations emerges:

As shown in Ref. 4 the low-lying multiplets of the $sl(2|1)$ symmetric chain ($\gamma \to 0$) are the singlet ground state with $E = 0$ in the normalization used here followed by a single $sl(2|1)$ octet as the lowest excitation. Above these there are two more degenerate octets and a pair of degenerate indecomposables, each containing 8 states. Upon deformation the degeneracies of these excitations lifted as described above, see Fig. 3. Note that the $s_3 = 1$ doublet arising from the lowest octet is part of the XXZ spin-1 subsector of the spectrum which according to Eq. (3.15) has a finite size
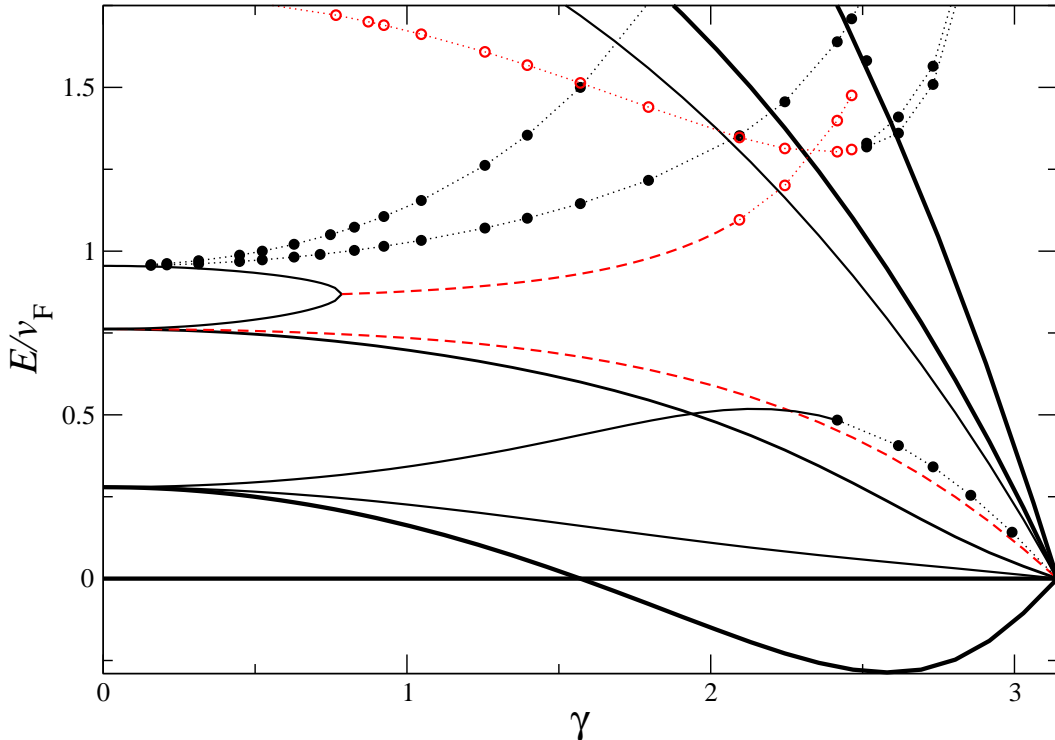
FIG. 3. Low energy part of the spectrum of the $L = 3$ chain for anisotropy $0 \leq \gamma < \pi$: black lines and filled symbols denote the real eigenvalues, red lines and open symbols the real part of complex eigenvalues of the Hamiltonian. Full and dashed lines denote eigenvalues obtained by solution of the Bethe equations, see Table I, whereas the symbols are eigenvalues obtained by numerical diagonalization of the Hamiltonian for which the corresponding configuration of Bethe roots has not been identified. Dotted lines connecting numerical data are guides to the eye only.

energy gap $\Delta E^{(XXZ)} = (2\pi v_F/L) \left[X_c - \frac{1}{8} \right]$ in the large L limit. For $\pi/2 < \gamma < \pi$ this doublet is the ground state of the mixed chain, as expected from the analysis of the XXZ-1 chain with anti-periodic boundary conditions for odd L. As $\gamma \to \pi$ all states evolving from this octet degenerate at $E = 0$.

The 16 states of the degenerate octets split into a quartet and an octet with real energies and two doublets with complex conjugate eigenvalues of the Hamiltonian. The latter eigenvalues also approach 0 as $\gamma \to \pi$. Similarly the states of the degenerate indecomposables split into two quartets and an octet, all with real energies. Increasing γ beyond $\approx \pi/4$ the real octets from these two groups degenerate and turn into two octets with complex conjugate energies. Our numerical data indicate that this conversion of pairs of real eigenvalues into pairs of complex conjugate ones appears in several regions of the spectrum. We have not been able to study whether this phenomenon persists as the system size L is increased, but it is a common feature in non-unitary models.
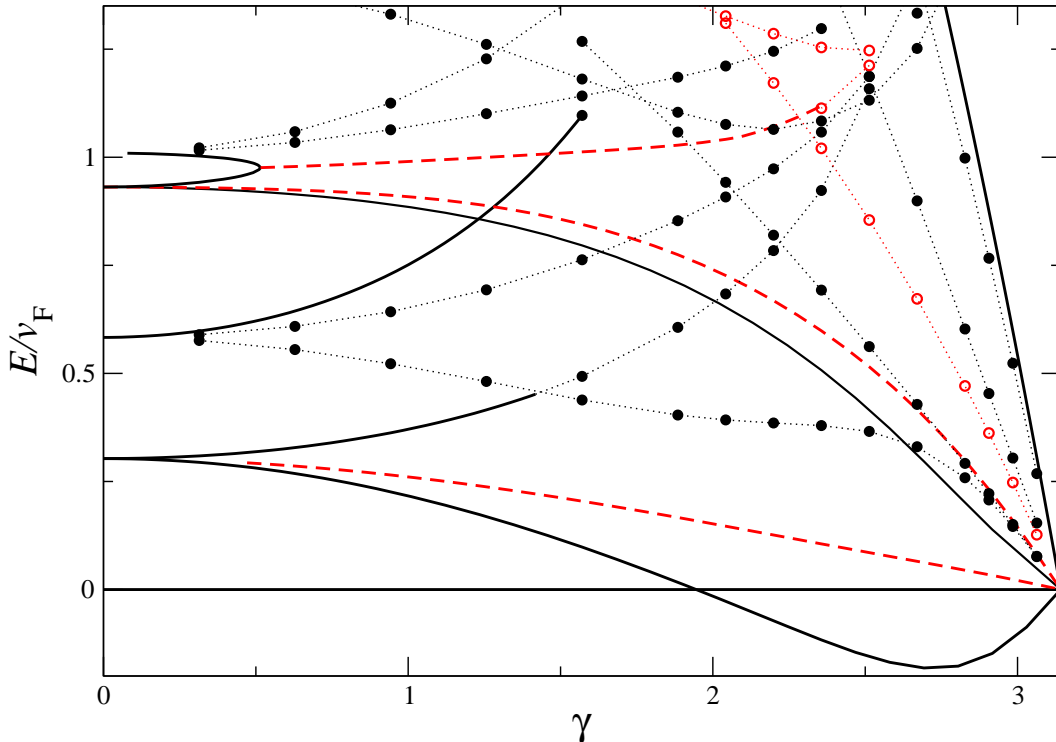
FIG. 4. Same as Fig. 3 but for $L = 4$.

In Figure 4 we present our data for the γ dependence of the low energy spectrum of the $L = 4$ mixed superspin chain. As $\gamma \to 0$ the spectrum (ordered by energy) consists of the $E = 0$ singlet ground state, two degenerate octets, an 8-dimensional indecomposable and another pair of degenerate octets [4]. The observed splittings and appearance of levels with complex conjugate eigenvalues fit into the scheme discussed for $L = 3$ above.

B. Analysis of the finite size spectrum – antiferromagnetic regime

Due to the identification (3.8) of the spectrum of the XXZ spin-1 chain within that of the superspin chain we already know part of the finite size scaling amplitudes – relative to the $E = 0$ eigenstate – in the latter:

$$\Delta E^{(mix)} = \frac{2\pi v_F}{L} \left(2 X_{(r,j)}^{(n,m)}(\gamma) - \frac{1}{4} \right) . \tag{4.4}$$

In translating the energies from the XXZ model we have used that as a consequence of (3.7) the Fermi velocity remains the same, $v_F^{(mix)} = v_F = 2\pi/\gamma$, and therefore the scaling dimensions of the superspin chain are twice of those given in (3.12) for the composite fields in the XXZ spin-1 chain. This is in agreement with the observations in Ref. 4.

For $\gamma < \pi/2$ the ground state is the unique state with $E_0(L) = 0$, hence the central charge of the model is

$$c = -\frac{6L}{\pi v_F} E_0 = 0\,, \qquad 0 \leq \gamma < \frac{\pi}{2}\,. \tag{4.5}$$

The lowest excitation corresponds to the conformal operator with scaling dimension $X_{(0,0)}^{(1,0)} = X_c$ in the π-twisted XXZ spin chain of odd length L (3.15). In the mixed chain this translates into a scaling dimension with scaling dimension $2X_c - 1/4 = (\pi - 2\gamma)/4\pi$ according to (4.4).

In the superspin chain this state is realized by $(L-1)/2$ narrow 2-strings. As mentioned above, a narrow string may be viewed as degeneration of two strange 2-strings of opposite type. Excitations can be created by lifting this degeneracy into configurations with different number of the two possible types of strange 2-strings, i.e. type '+'-strings with $\lambda^{(1)} = (\lambda^{(2)})^* = \lambda + i\gamma/4$ and '−'-strings with $\lambda^{(1)} = (\lambda^{(2)})^* = \lambda - i\gamma/4$. The narrow string state is described by the same number of $\pm$ strange strings, $\Delta N = N_+ - N_- = 0$. Similar as in Ref. 4 one can show that states with different but finite ΔN have the same energy in the thermodynamic limit (note, however, that configurations with ΔN even (odd) are only possible for L odd (even)). Computing the energies of these states we find a logarithmic fine structure on top of the level corresponding to the operator $(n,m) = (1,0)$, i.e.

$$\frac{L}{2\pi v_F}\Delta E^{(mix)} = \frac{\pi - 2\gamma}{4\pi} + K(\gamma, L)(\Delta N)^2\,, \tag{4.6}$$

see Fig. 5 for $\gamma = 2\pi/7$. We have also displayed the L-dependence of the $\Delta N = 0$ level corresponding to the twisted spin chain excitation with $(n,m) = (0,1)$ for even L (3.14): this state leads to a scaling dimension $\frac{1}{4}(\pi + \gamma)/(\pi - \gamma)$ in the spectrum of the mixed superspin chain and is part of the lowest $sl(2|1)$ indecomposable for even L as $\gamma \to 0$.

Starting from a non-linear sigma model with a supersphere as target space Ikhlef *et al.* [6] have proposed that this logarithmic fine structure in the finite size spectrum is the signature of a non-compact boson in the continuum theory. At intermediate scales, given by the size L of the lattice regularization, the renormalization of the coupling constant leads to an effective radius of the non-compact boson given as

$$(R_{nc})^2 \propto \frac{1}{A(\gamma)}\left[\ln(L/L_0)\right]^2\,. \tag{4.7}$$

This, in turn, generates the logarithmic structure (4.6) observed in the numerical data:

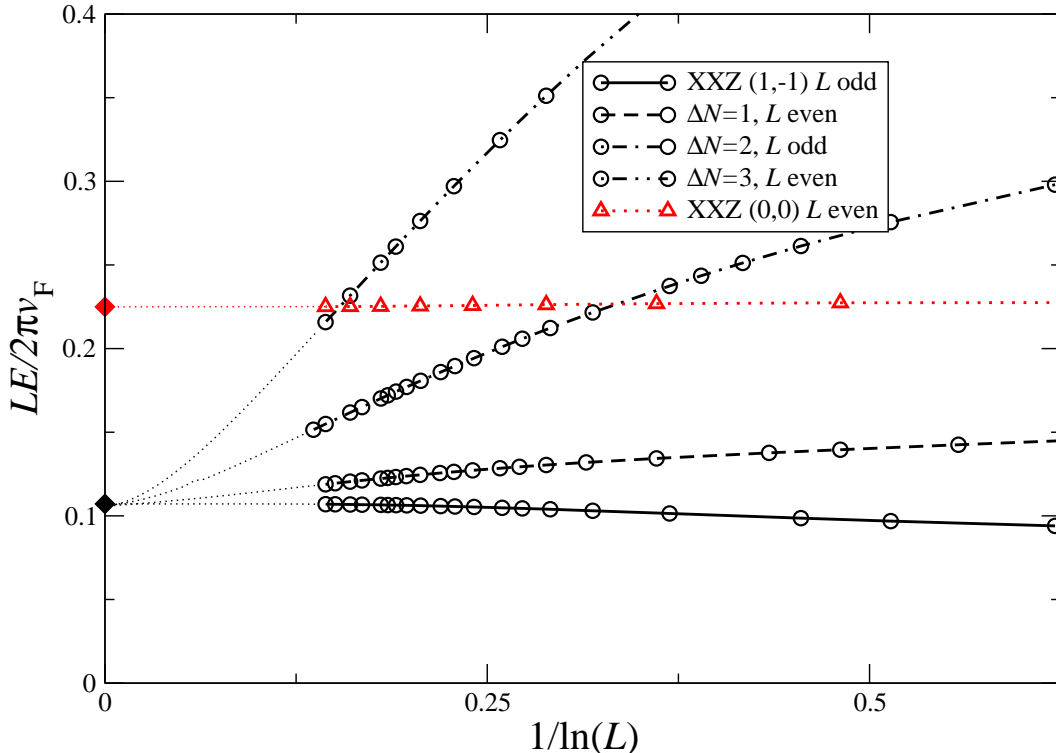$$K(\gamma, L) = \frac{A(\gamma)}{\ln(L/L_0)^2} \tag{4.8}$$

FIG. 5. Evolution of the fine structure of the low energy spectrum of the mixed spin chain as a function of L for $\gamma = 2\pi/7$: circles denote energies scaling to the $(n, m) = (1, -1)$ level of the XXZ spin chain with odd length, triangles denote the $(0, 0)$ level of the XXZ chain. The dotted lines connecting to $L = \infty$ are rational function extrapolations of the numerical data.

In Fig. 6 we present numerical estimates of the amplitude $A(\gamma)$ for the lowest excitation based on the finite size spectrum for system sizes up to $L = 4095$. We find that the amplitude is well described by

$$A(\gamma) = \frac{5}{2} \frac{\pi - \gamma}{\pi + \gamma}. \tag{4.9}$$

For $\gamma \gtrsim 1$ the extrapolation of the numerical data is within 1% of this conjecture. For more convincing evidence, in particular at small values of the deformation parameter γ, one would need additional information about higher order corrections to (4.8) and have to study system sizes which are out of reach for this method based on the numerical solution of the Bethe equations (2.17).

For $\pi/2 < \gamma < \pi$ the set of levels (4.6) has energies below the $E \equiv 0$ eigenstate of the mixed chain for L sufficiently large, see Fig. 7. As a consequence the model is in a different universality class with central charge determined by the finite size scaling behaviour of the lowest level in this set, i.e.

$$c_{\text{eff}}(\gamma) = -\frac{6L}{\pi v_F} E^{(mix)} = 3 \frac{2\gamma - \pi}{\pi}, \qquad \frac{\pi}{2} < \gamma < \pi. \tag{4.10}$$
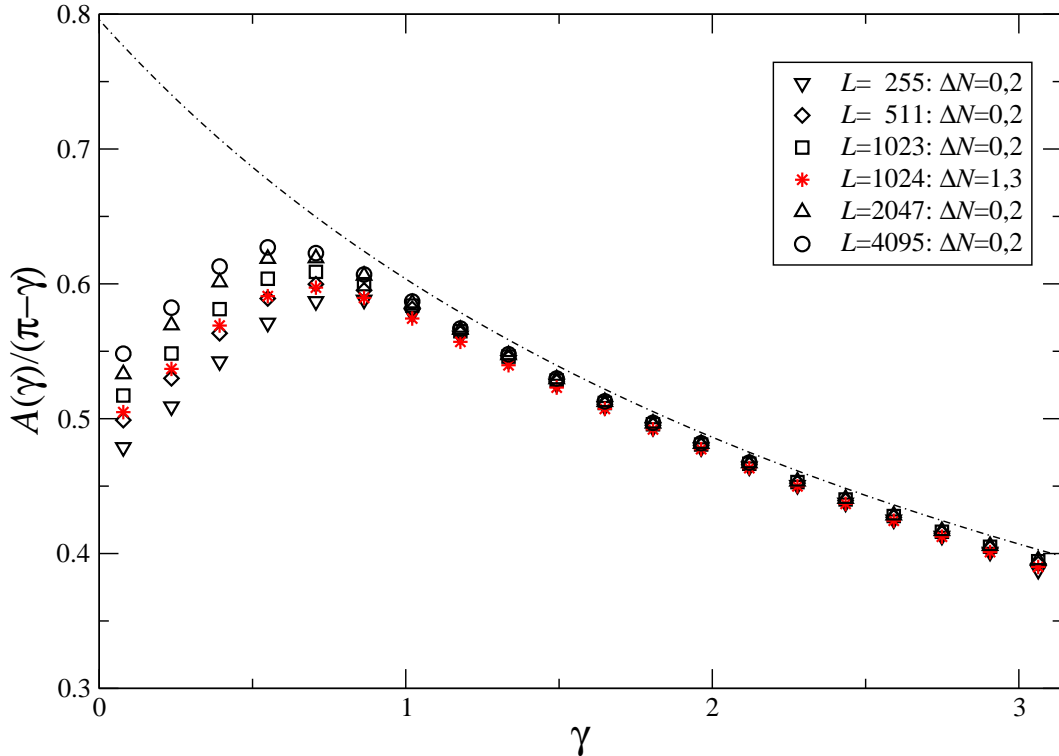
FIG. 6. Amplitude of the logarithmic fine structure extracted from comparison of the energies of corresponding states at sizes $L = 2L' + 1$ ($2L'$ for L even) and L'. The line is the conjectured γ-dependence Eq. (4.9).

Note that this state can be identified with the lowest level of the XXZ spin-1 chain for odd L only. For even L its realization in the mixed superspin is in terms of a strange string configuration with $\Delta N = \pm 1$. Immediately above this ground state there is a continuum of states with energy gaps vanishing as $\propto (\Delta N)^2 / \left[L \ln(L/L_0)^2 \right]$ due to the presence of the non-compact boson: our finite size analysis indicates that these gaps show the same γ dependence as in (4.9) given above. The first excitation from the XXZ spin-1 subset of the spectrum above this continuum is the $E \equiv 0$ state corresponding to a scaling dimension

$$X = \frac{2\gamma - \pi}{4\pi}. \tag{4.11}$$

V.   FERROMAGNETIC REGIME OF THE MIXED CHAIN

Again we use the spectral relation (2.19) to discuss the properties of the mixed superspin chain in this regime in the interval $0 \le \gamma < \pi$ by changing the sign of the energy eigenvalues (2.18).

As for the antiferromagnetic regime above we begin our analysis based on numerical data for the
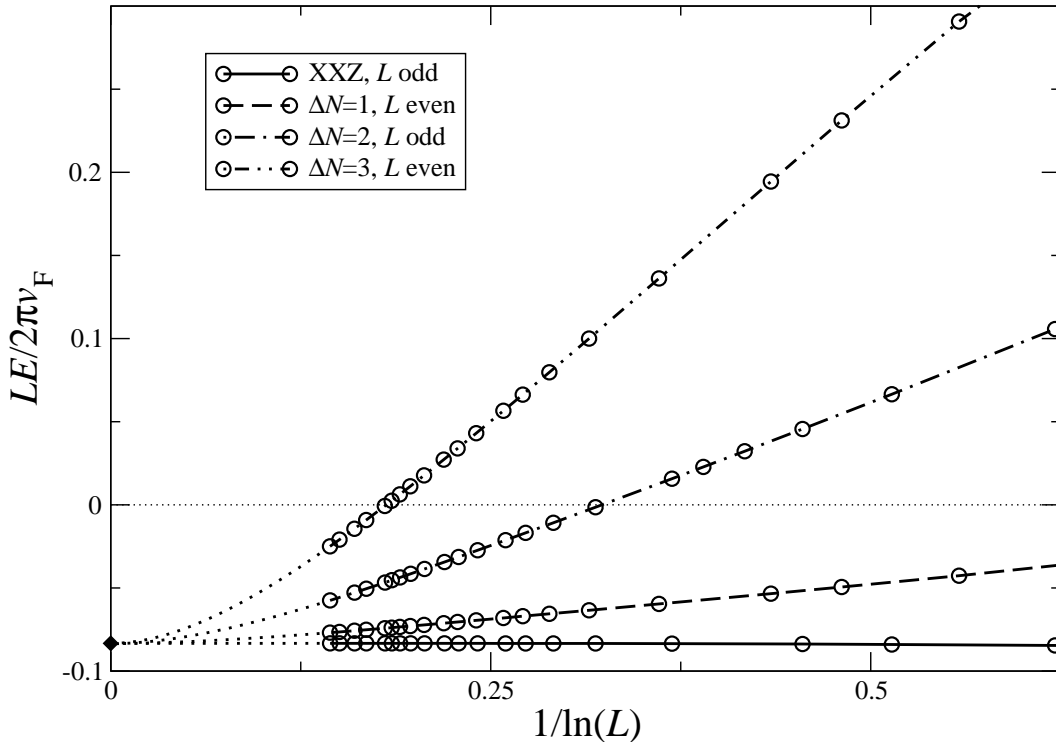
FIG. 7. As Fig. 5 but for $\gamma = 2\pi/3$. The dotted line denotes the energy level at $E = 0$ of the singlet state without any finite size scaling in the spectrum of the mixed chain for L both even and odd.

spectrum of the $L = 3$ chain obtained by exact diagonalization of the superspin Hamiltonian, see Table II for $\gamma = 2\pi/7 < \pi/3$: according to our discussion of the disordered ferromagnetic regime of the XXZ spin-1 chain above the lowest state from the XXZ spin-1 part of the spectrum for this value of γ is the completely polarized reference state with $s_3 = 3$ and energy $E = -12\cot(\gamma/2)$ according to (3.8). In Table II we have also listed the level corresponding to the primary field $(n, m) = (0, \frac{1}{2})$ in the twisted XXZ model (3.16).

The numerical data reveal that below the reference state of the XXZ spin chain there are many states with lower energies in the spectrum of the mixed superspin chain in the charge-sectors $b = 0, \pm 1/2$ and with magnetization $0 \leq s_3 \leq L$: the corresponding Bethe configurations consist of (N_1, N_2) roots with $N_1 - N_2 = 0, \pm 1$ and $Im(\lambda_j^{(a)}) = \pi/2$, i.e. $(1, -)$-strings. The ground state in the sector $(L, L - 1)$ (together with the equivalent sector $(L - 1, L)$) is four-fold degenerate.

TABLE II. Low energy states of the $L = 3$ superspin chain in the ferromagnetic regime for $\gamma = 2\pi/7$ and the identified Bethe configurations.

(N_1, N_2)	Energy E	degeneracy	Bethe roots
$(3, 2)$	-27.8683	4	$\Lambda^{(1)} = \{\pm 1.1935 + i\pi/2, \, i\pi/2\}$, $\Lambda^{(2)} = \{\pm 0.4797 + i\pi/2\}$
$(3, 3)$	-27.7508	2	$\Lambda^{(1)} = \{-0.7367 + i\pi/2, \, 0.2722 + i\pi/2, \, \infty\} = -\Lambda^{(2)}$
$(2, 2)$	-27.4205	4	$\Lambda^{(1)} = \{-1.0384 + i\pi/2, \, 0.2015 + i\pi/2\} = -\Lambda^{(2)}$
$(2, 1)$	-27.1935	4	$\Lambda^{(1)} = \{\pm 0.5829 + i\pi/2\}$, $\Lambda^{(2)} = \{i\pi/2\}$
$(1, 1)$	-26.4469	4	$\Lambda^{(1)} = \{-0.4447 + i\pi/2\} = -\Lambda^{(2)}$
$(1, 0)$	-25.8814	4	$\Lambda^{(1)} = \{i\pi/2\}$
$(0, 0)$	-24.9183	2	(XXZ pseudo vacuum)
$(3, 2)$	-24.8425	8	$\Lambda^{(1)} = \{-1.0326 + i\pi/2, \, 0.3894 + i\pi/2, \, 0.6432\}$
			$\Lambda^{(2)} = \{-0.2736 + i\pi/2, \, 0.7440\}$
$(3, 3)$	-24.7595	4	$\Lambda^{(1)} = \{-0.5477 + i\pi/2, \, 1.0369, \, \infty\}$
			$\Lambda^{(2)} = \{-\infty, \, -0.0189 + i\pi/2, \, 0.5909\}$
$(2, 2)$	-24.6243	8	$\Lambda^{(1)} = \{-0.8222, \, -0.2226 + i\pi/2\}$
			$\Lambda^{(2)} = \{-0.7559, \, 0.8563 + i\pi/2\}$
$\vdots$			
$(3, 3)$	-23.6547	2	$\Lambda^{(1)} = \{0.6023 \pm i0.6800, \, 0.7226\} = \Lambda^{(2)}$ (XXZ)

A. Thermodynamic limit

Based on this observation we shall now study this ground state in the thermodynamic limit $L \to \infty$. To make further progress it is convenient to rewrite the rapidities $\lambda_j^{(a)}$ as,

$$\lambda_j^{(a)} = \mu_j^{(a)} + i\frac{\pi}{2}, \tag{5.1}$$

where $\mu_j^{(a)} \in \mathbb{R}$ for $a = 1, 2$. Now, by substituting Eq. (5.1) in the Bethe ansatz equations (2.17) and by taking their logarithms we find that the resulting relations for $\mu_j^{(k)}$ are,

$$L\Phi(\mu_j^{(1)}, \gamma - \pi) = 2\pi Q_j^{(1)} + \sum_{k=1}^{N_2} \Phi(\mu_j^{(1)} - \mu_k^{(2)}, \gamma), \qquad j = 1, \ldots, N_1$$

$$L\Phi(\mu_j^{(2)}, \gamma - \pi) = 2\pi Q_j^{(2)} + \sum_{k=1}^{N_1} \Phi(\mu_j^{(2)} - \mu_k^{(1)}, \gamma), \qquad j = 1, \ldots, N_2 \tag{5.2}$$

where $\Phi(x, \gamma) = 2 \arctan(\tanh(x) \cot(\gamma/2))$. The numbers $Q_j^{(a)}$ define the many possible branches of the logarithm. They have to be chosen integer or half-odd integer depending on the parities of N_a according to the rule

$$Q_j^{(1)} \equiv \frac{N_2}{2} \mod 1, \qquad Q_j^{(2)} \equiv \frac{N_1}{2} \mod 1. \tag{5.3}$$

For example the ground state in the sector $N_1 = L$ and $N_2 = L - 1$ is described by the symmetric sequences

$$Q_j^{(1)} = \frac{L+1}{2} - j, \qquad j = 1, \ldots, L,$$
$$Q_j^{(2)} = \frac{L}{2} - j, \qquad j = 1, \ldots, L-1.$$
(5.4)

At this point we have the basic ingredients to compute some of the thermodynamic limit properties. When $L \to \infty$ the number of roots $\mu_j^{(a)}$ tend towards a continuous distribution on the real axis whose density which we shall denote by $\rho^{(a)}(\mu)$. The Bethe equations (5.2) turn into coupled linear integral relations for the densities $\rho^{(a)}(\mu)$ which can be solved by Fourier transform. The fact that Eqs. (5.2) are symmetric under the exchange of rapidities $\mu_j^{(1)} \leftrightarrow \mu_j^{(2)}$ in the thermodynamic limit implies that $\rho^{(1)}(\mu) \equiv \rho^{(2)}(\mu)$. The final result for such density is,

$$\rho^{(a)}(\mu) = \frac{1}{(\pi - \gamma/2)} \frac{\cos\left[\frac{\pi\gamma}{4(\pi-\gamma/2)}\right] \cosh\left[\frac{\pi\mu}{\pi-\gamma/2}\right]}{\cosh\left[\frac{2\pi\mu}{\pi-\gamma/2}\right] + \cos\left[\frac{\pi\gamma}{2(\pi-\gamma/2)}\right]}, \qquad \text{for } a = 1, 2.$$
(5.5)

Now from the expressions for the density $\rho^{(a)}(\mu)$ and Eq. (2.18) we can compute the ground state energy density $\tilde{e}_\infty = E_0/L$. By writing the infinite volume limit of Eq. (2.18) in terms of its Fourier transform we find

$$\tilde{e}_\infty = -4\cot(\gamma/2) - 4\int_0^\infty d\omega \frac{\sinh[\omega\gamma/2]\cosh[\omega\gamma/4]}{\sinh[\omega\pi/2]\cosh[\omega(2\pi-\gamma)/4]} \qquad \text{for } 0 \le \gamma < \pi.$$
(5.6)

In addition, we have verified that the low-lying excited states about the ground state are gapless. As usual, these states can be obtained by inserting holes in the density distribution of $\mu_j^{(a)}$ by making alternative choices for $Q_j^{(a)}$. This procedure is nowadays familiar to many integrable models solved by Bethe ansatz and for technical details see for example ([36–38]). We find that the low-momenta dispersion relation among the energy $\epsilon^{(a)}(\mu)$ and momenta $p^{(a)}(\mu)$, both measured from the ground state, has a relativistic behaviour

$$\epsilon^{(a)}(\mu) \sim \tilde{v}_F^{(mix)} p^{(a)}(\mu)$$
(5.7)

The common slope at $p^{(a)}(\mu) = 0$ is the corresponding Fermi velocity of the excitations. It is determined by

$$\tilde{v}_F^{(mix)} = \left.\frac{\dot{\epsilon}^{(a)}(\mu)}{2\pi\rho^{(a)}(\mu)}\right|_{\mu=\infty} = \frac{2\pi}{2\pi - \gamma}.$$
(5.8)

As expected from (3.7) it coincides with the velocity $\tilde{v}_F$ of low energy excitations of the XXZ spin-1 chain in the disordered ferromagnetic regime, see Section III B.

B.   Analysis of the finite size spectrum – ferromagnetic regime

From our investigation of the behaviour of the Bethe ansatz roots associated to the low-lying excitations we found that they can be well described in terms of real rapidities. The roots with fixed imaginary part at $i\frac{\pi}{2}$ can easily be mapped on real roots by means the straightfoward shift (5.1). We remark however that some excitations have the peculiar feature that some of the their roots have the real part located at infinity. This scenario suggests us that a first insight on the structure of the finite-size corrections can be obtained by applying the standard density root method, see for instance [38–42]. This technique explores the Bethe ansatz solution and it allows to compute the $O\left(L^{-2}\right)$ corrections to the densities of roots $\rho^{(k)}(\mu)$. This approach predicts that the finite-size corrections to the low-lying energies eigenvalues have the following form,

$$E(L,\gamma) - L\tilde{e}_\infty = \frac{2\pi\tilde{v}_F}{L}\left[-\frac{1}{6} + X_{n_1,n_2}^{m_1,m_2}(\gamma)\right] + o\left(L^{-1}\right), \tag{5.9}$$

where the scaling dimensions $X_{n_1,n_2}^{m_1,m_2}(\gamma)$ depend on the anisotropy γ as

$$\begin{aligned} X_{n_1,n_2}^{m_1,m_2}(\gamma) =&\frac{1}{4}\left(1 - \frac{\gamma}{2\pi}\right)(n_1 - n_2)^2 + \frac{1}{4}\left(1 - \frac{\gamma}{2\pi}\right)^{-1}(m_1 - m_2)^2 \\ &+ \frac{1}{4}\left(\frac{\gamma}{2\pi}\right)(n_1 + n_2)^2 + \frac{1}{4}\left(\frac{2\pi}{\gamma}\right)(m_1 + m_2)^2. \end{aligned} \tag{5.10}$$

In (5.10) the integers n_1 and n_2 are related to the number of roots at each level of the Bethe equations by $N_1 = L - n_1$ and $N_2 = L - n_2$. Therefore $(n_1 \pm n_2)/2$ are associated to the conserved $U(1)$ spin s_3 and charge b of the model: the scaling dimensions (5.10) exhibit exact spin charge separation in the low energy effective theory. The corresponding excitations of the model are free bosons with compactification radii $R_s^2 \sim \gamma/2\pi$ and $R_h^2 \sim (1 - \gamma/2\pi)$, usually denominated spinon and holon modes.[1] The indices m_1 (m_2) are related to macroscopic momentum of the excitation due to backscattering processes on the first (second) level of the Bethe ansatz and they are usually called vortex excitations. As a consequence of (5.3) they take integer (half-odd integer) values depending on the parity of $N_1 + N_2$ leading to the following constraint connecting spinon and vortex numbers:

- for $n_1 \pm n_2$ odd $\rightarrow$ $m_1, m_2 = 0, \pm 1, \pm 2, \ldots$

- for $n_1 \pm n_2$ even $\rightarrow$ $m_1, m_2 = \pm\dfrac{1}{2}, \pm\dfrac{3}{2}, \pm\dfrac{5}{2}, \ldots$.

$$\tag{5.11}$$

Let us now investigate the validity of the formulae (5.10) for the conformal dimensions together with the selection rule (5.11). In order to do that we have solved the Bethe ansatz equations for a

---

[1] A similar observation has been made in one of the critical phases of a Temperley Lieb model with staggered spectral parameters where the effective field theory consists of a compact boson and two Majorana fermions [43]. In this model, however, the low energy degrees of freedom cannot be related to $U(1)$ charges of the microscopic model.

TABLE III. Finite size sequences 5.12 of the anomalous dimension $X_{1,0}^{0,0}(\gamma)$ for $\gamma = \pi/6$, $\pi/3$, $\pi/2$, $2\pi/3$ from the Bethe ansatz. The expected exact conformal dimension is $X_{1,0}^{0,0}(\gamma) = \frac{1}{4}$.

$X_{1,0}^{0,0}(\gamma)$	$\frac{\pi}{6}$	$\frac{\pi}{3}$	$\frac{\pi}{2}$	$\frac{2\pi}{3}$
4	0.20487467	0.23017601	0.24810873	0.24554137
8	0.23375071	0.24621304	0.24978827	0.24940359
12	0.24319443	0.24843089	0.24992216	0.24976865
16	0.24643218	0.24913601	0.24995927	0.24987579
20	0.24780188	0.24945223	0.24997482	0.24992223
24	0.24850243	0.24962151	0.24998285	0.24994660
28	0.24891117	0.24972275	0.24998754	0.24996104
32	0.24917161	0.24978814	0.24999053	0.24997031
Extrap.	0.2503(2)	0.250003(1)	0.250002(2)	0.250001(2)
Exact	0.25	0.25	0.25	0.25

number of low-lying states up to $L = 32$. From the numerical data we compute the sequence

$$X(L) = \frac{L}{2\pi\tilde{v}_F}\left(E(L,\gamma) - L\tilde{e}_\infty\right) + \frac{1}{6} \tag{5.12}$$

which in the thermodynamic limit is expected to extrapolate to the dimensions (5.10).

In Table III we show the finite-size sequences (5.12) for the ground state $E_0(L,\gamma)$ in the case of various values of γ. The extrapolated value of the corresponding conformal dimension turns out to be independent of the anisotropy γ whose value is in good accordance with the one predicted by Eq. (5.10) for $X_{1,0}^{0,0}(\gamma) = X_{0,1}^{0,0}(\gamma) \equiv \frac{1}{4}$. From this result we find that the ground state energy scales as

$$E_0(L,\gamma) - L\tilde{e}_\infty = \frac{\pi v_F}{6L} + o\left(L^{-1}\right), \tag{5.13}$$

which leads us to conclude that the continuum limit of the superspin chain in the disordered ferromagnetic regime should be described by a conformally invariant theory with central charge $c = -1$. The respective anomalous dimensions $\bar{X}_{n_1,n_2}^{m_1,m_2}(\gamma)$ of the theory have to be measured from the ground state (5.13) and therefore they should be given by,

$$\bar{X}_{n_1,n_2}^{m_1,m_2}(\gamma) = X_{n_1,n_2}^{m_1,m_2}(\gamma) - \frac{1}{4}. \tag{5.14}$$

We have also analyzed the corrections to scaling due to the presence of irrelevant operators in the lattice Hamiltonian [44]. For all values of γ we found the leading corrections to the finite size estimate (5.12) for $X_{0,1}^{0,0}(\gamma)$ to be of order L^{-2} arising from the conformal block of the identity operator which explains the good convergence of the extrapolation.

TABLE IV. Finite size sequences 5.12 of the anomalous dimension $X_{0,0}^{\frac{1}{2},-\frac{1}{2}}(\gamma)$ for $\gamma = \pi/6$, $\pi/3$, $\pi/2$, $2\pi/3$ from the Bethe ansatz. The expected exact conformal dimension is $X_{0,0}^{\frac{1}{2},-\frac{1}{2}}(\gamma) = \pi/(4\pi - 2\gamma)$.

$X_{0,0}^{\frac{1}{2},-\frac{1}{2}}(\gamma)$	$\frac{\pi}{6}$	$\frac{\pi}{3}$	$\frac{\pi}{2}$	$\frac{2\pi}{3}$
4	0.23109569	0.28352514	0.33170562	0.36094436
8	0.25745093	0.29695955	0.33325340	0.37254539
12	0.26633674	0.29875319	0.33331810	0.37397623
16	0.26938340	0.29931576	0.33332857	0.37443588
20	0.27066931	0.29956684	0.33333139	0.37464230
24	0.27132594	0.29970094	0.33333245	0.37475283
28	0.27170870	0.29978104	0.33333283	0.37481895
32	0.27211767	0.29983274	0.33333303	0.37486165
Extrap.	0.27273(2)	0.300004(2)	0.3333332(2)	0.375001(2)
Exact	0.272727 ...	0.3	0.333333 $\cdots$	0.375

We now turn our attention to the excited states in order to bring extra support to the proposal (5.10), (5.11). The first excitation above the ground state (5.13) occurs in the sector $n_1 = n_2 = 0$. Our analysis of the $L = 3$ system (see Table II) indicates that among the corresponding Bethe roots there is a pair of rapidities $(\lambda^{(1)}, \lambda^{(2)})$ which takes values $(\pm\infty, \mp\infty)$. The presence of such infinities leads to an effective scattering phase shift of $\exp[\pm i\gamma]$ for the remaining roots. Due to this peculiarity we shall present explicitly the form of the Bethe equations for the finite roots

$$L\Phi(\mu_j^{(1)}, \gamma - \pi) = 2\pi Q_j^{(1)} + \gamma + \sum_{k=1}^{L-2} \Phi(\mu_j^{(1)} - \mu_k^{(2)}, \gamma), \qquad j = 1, \ldots, L-1$$

$$L\Phi(\mu_j^{(2)}, \gamma - \pi) = 2\pi Q_j^{(2)} - \gamma + \sum_{k=1}^{L-1} \Phi(\mu_j^{(2)} - \mu_k^{(1)}, \gamma), \qquad j = 1, \ldots, L-1.$$

(5.15)

For this state the numbers $Q_j^{(a)}$ are given by

$$Q_j^{(1)} = \frac{L+1}{2} - j, \qquad j = 1, \ldots, L-1,$$

$$Q_j^{(2)} = -\frac{L+1}{2} + j, \qquad j = 1, \ldots, L-1.$$

(5.16)

In table (IV) we present the finite-size estimates associated to the state described by Eqs. (5.15) with (5.16). We observe that the the extrapolated values agree with the proposal (5.10), (5.11) which predicts that the lowest conformal dimension is $\bar{X}_{0,0}^{\frac{1}{2},-\frac{1}{2}}(\gamma) = \frac{\gamma}{4(2\pi-\gamma)}$.

In Tables V-VIII we present the finite-size sequences for several low-lying excitations in other sectors. We observe that the extrapolated values corroborate the result predicted by (5.10).

TABLE V. Finite size sequences 5.12 of the anomalous dimension $X_{1,1}^{\frac{1}{2};-\frac{1}{2}}(\gamma)$ for $\gamma = \pi/6$, $\pi/3$, $\pi/2$, $2\pi/3$ from the Bethe ansatz. The expected exact conformal dimension is $X_{1,1}^{\frac{1}{2};-\frac{1}{2}}(\gamma) = \frac{\gamma}{2\pi} + \frac{\pi}{2(2\pi-\gamma)}$.

$X_{1,1}^{\frac{1}{2};-\frac{1}{2}}(\gamma)$	$\frac{\pi}{6}$	$\frac{\pi}{3}$	$\frac{\pi}{2}$	$\frac{2\pi}{3}$
4	0.31054918	0.44669719	0.58683657	0.74133601
8	0.33974964	0.46283122	0.58433551	0.71638581
12	0.34923933	0.46507338	0.58378663	0.71189057
16	0.35248317	0.46578873	0.58358979	0.71032924
20	0.35385561	0.46610987	0.58349789	0.70960905
24	0.35455798	0.46628188	0.58344777	0.70921857
28	0.35496794	0.46638478	0.58341748	0.70898230
32	0.35522923	0.46645125	0.58339779	0.70883087
Extrap.	0.35603(2)	0.466665(2)	0.5833334(1)	0.708332(2)
Exact	0.356060 ...	0.466666 $\cdots$	0.583333 $\cdots$	0.708333 $\cdots$

TABLE VI. Finite size sequences 5.12 of the anomalous dimension $X_{1,2}^{0,0}(\gamma)$ for $\gamma = \pi/6$, $\pi/3$, $\pi/2$, $2\pi/3$ from the Bethe ansatz. The expected exact conformal dimension is $X_{1,2}^{0,0}(\gamma) = \frac{1}{4} + \gamma/\pi$

$X_{1,2}^{0,0}(\gamma)$	$\frac{\pi}{6}$	$\frac{\pi}{3}$	$\frac{\pi}{2}$	$\frac{2\pi}{3}$
4	0.36660004	0.56006032	0.75496874	0.95242531
8	0.39901997	0.57907838	0.75200345	0.92788809
12	0.40929983	0.58158419	0.75094335	0.92183973
16	0.41280124	0.58237304	0.75054074	0.91961495
20	0.41428312	0.58272535	0.75034904	0.91856536
24	0.41504200	0.58291356	0.75024350	0.91798979
28	0.41548512	0.58302599	0.75017939	0.91764084
32	0.41576759	0.583098552	0.75013758	0.91741358
Extrap.	0.4166(2)	0.583332(1)	0.750001(2)	0.916662(2)
Exact	0.41666 $\cdots$	0.58333 $\cdots$	0.75	0.91666 $\cdots$

Of rather special nature is the state considered in Table VIII: this is the lowest excitation from the XXZ spin-1 part of the spectrum. As in the antiferromagnetic regime the finite size scaling of these states can be deducted using the spectral relation (3.8). Using the same reasoning as above the scaling dimensions $\tilde{X}_{n,m}(\gamma)$ of the spin-1 chain in the ferromagnetically disordered regime, Eq. (3.16), should appear doubled in the spectrum of scaling dimensions of the superspin chain. Comparison with (5.10) shows that this is indeed true (remember that m in (3.16) takes half-odd

TABLE VII. Finite size sequences 5.12 of the anomalous dimension $X_{1,0}^{1,-1}(\gamma)$ for $\gamma = \pi/6$, $\pi/3$, $\pi/2$, $2\pi/3$ from the Bethe ansatz. The expected exact conformal dimension is $X_{1,0}^{1,-1}(\gamma) = \frac{1}{4} + \frac{2\pi}{(2\pi-\gamma)}$.

$X_{1,0}^{1,-1}(\gamma)$	$\frac{\pi}{6}$	$\frac{\pi}{3}$	$\frac{\pi}{2}$	$\frac{2\pi}{3}$
4	2.78965545	1.76360998	1.5577620	1.59077025
8	1.99919576	1.58255107	1.5863263	1.70990754
12	1.69307777	1.51547069	1.5856105	1.73214654
16	1.55596049	1.48826402	1.5848095	1.73994982
20	1.48454418	1.47493397	1.5843369	1.74356556
24	1.44315270	1.46748697	1.5840527	1.74553075
28	1.41720088	1.46292463	1.5838718	1.74671607
32	1.39992651	1.45993403	1.5837506	1.7474855
Extrap.	1.3404(3)	1.45003(1)	1.5834(2)	1.75002(1)
Exact	$1.340909\cdots$	1.45	$1.58333\cdots$	1.75

TABLE VIII. Finite size sequences 5.12 of the anomalous dimension $X_{0,0}^{\frac{1}{2},\frac{1}{2}}(\gamma)$ for $\gamma = 2\pi/7$, $2\pi/5$, $2\pi/3$, $5\pi/6$ from the Bethe ansatz. The expected exact conformal dimension is $X_{0,0}^{\frac{1}{2},\frac{1}{2}}(\gamma) = \frac{\pi}{2\gamma}$.

$X_{0,0}^{\frac{1}{2},\frac{1}{2}}(\gamma)$	$\frac{2\pi}{7}$	$\frac{2\pi}{5}$	$\frac{2\pi}{3}$	$\frac{5\pi}{6}$
4	1.84589078	1.29492470	0.75018486	0.54556892
8	1.76868129	1.25924483	0.75002911	0.58757296
12	1.75782587	1.25398066	0.75001177	0.59492733
16	1.75432209	1.25248723	0.75000640	0.59722733
20	1.75274406	1.25141093	0.75000403	0.59824616
24	1.75189751	1.25097723	0.75000277	0.59878935
28	1.75139056	1.25071683	0.75000203	0.59911369
32	1.75106290	1.25054825	0.75000154	0.59932298
Extrap.	1.75002(2)	1.25003(1)	0.7500002(3)	0.600003(1)
Exact	1.75	1.25	0.75	0.6

integer values for twist $\varphi = \pi$):

$$X_{n,n}^{m,m} = 2\tilde{X}_{n,m} = n^2 \frac{\gamma}{2\pi} + m^2 \frac{2\pi}{\gamma} \tag{5.17}$$

is exactly the pure spinon part of the low energy spectrum of the mixed superspin chain.

As an example, we have computed the finite size sequences (5.12) for the dimension $X_{0,0}^{\frac{1}{2},\frac{1}{2}}(\gamma) = \frac{\pi}{\gamma}$. This is the state discussed at the end of Section III B: its root configuration changes at $\gamma = \pi/k$, $k = 2, 3, \ldots$ evolving into single narrow string of L roots on both levels of the Bethe ansatz for

$\gamma < \pi/L$.

In the isotropic limit, $\gamma \to 0$, this state is an $sl(2|1)$-descendent of the (completely polarized) reference state of the superspin chain with charges $(b, s_3) = (0, L)$ and lies outside of the low energy part of the spectrum. Unlike the XXZ spin-1 chain the superspin chain remains conformal in the isotropic limit of the disordered ferromagnetic regime: the holon sector, i.e. states from (5.9), (5.10) with $m_1 = -m_2$, remains conformal for $\gamma = 0$. Taking into account (5.11) their scaling dimensions are

$$
X_{n_1,n_2}^{m_1,-m_1}(0) = \begin{cases} \frac{1}{4}(2n+1)^2 + m^2 & \text{if } n_1 - n_2 = 2n + 1 \text{ and } m_1 = m, \\ n^2 + \frac{1}{4}(2m+1)^2 & \text{if } n_1 - n_2 = 2n \text{ and } m_1 = m + \frac{1}{2} \end{cases} \tag{5.18}
$$

with integer m. These are the conformal dimensions of the isotropic $osp(2|2)$ spin chain [5, 10, 11].

We have also studied the finite size scaling behaviour of several states with configurations which, apart from $(1, -)$ strings, contain real roots and inifinite roots on one or both levels (the existence of such configurations in the low energy sector of the ferromagnetic regime is indicated by our small system analysis, see e.g. Table II). In all cases we have considered these levels corresponded to descendents of the primary conformal fields identified before, i.e. with scaling dimensions $\bar{X}_{n_1,n_2}^{m_1,m_2} + n$ with integer n.

VI.   CONCLUSION

In this paper we have studied an integrable $U_q[sl(2|1)]$ vertex model built from alternating fundamental and dual three-dimensional representations first introduced by Gade [8]. Based on its solution by means of the algebraic Bethe ansatz we have computed the properties of this model in the thermodynamic limit and analyzed the finite size scaling of the low energy spectrum. From the latter we conclude that the critical point with central charge $c = 0$ of the undeformed model identified before [4] is stable against variation of the anisotropy γ: as long as $\gamma \in [0, \pi/2)$ the ground state energy vanishes exactly without any finite size effects. In the continuum limit we find that the model displays a continuous spectrum of exponents in the sector with $U_q[sl(2|1)]$-charge $b = 0$. As in the isotropic $sl(2|1)$ supersin chain the lower edges (4.4) of the continua can be identified with the scaling dimensions in an antiperiodically twisted spin-1 chain, in this case the Fateev-Zamolodchikov model. The continuous part of the conformal spectrum leads to a fine structure (4.6) in the spectrum of the large but finite superspin chain. This fine structure can be explained as signature of the presence of a non-compact degree of freedom in the continuum

theory with coupling constant renormalized to an intermediate scale of the order of the length L of the superspin chain. The γ-dependence of the coupling constant has been identified based on our numerical solution of the Bethe equations. At $\gamma = \pi/2$ a level crossing occurs changing the ground state and leading to an effective central charge taking values $0 \le c_{\text{eff}}(\gamma) < 3$ depending on the deformation parameter $\gamma \in [\pi/2, \pi)$. Again, this critical behaviour mirrors that of the XXZ spin-1 chain of odd length L in the antiferromagnetically disordered regime subject to antiperiodic twisted boundary conditions.

The spectrum in the ferromagnetic regime $\pi < \gamma \le 2\pi$ (or, equivalently, that of the chain with opposite sign of the exchange constant for anisotropies $\tilde{\gamma} = 2\pi - \gamma$) of the superspin chain is completely different: our finite size scaling analysis indicates that it is the same as for the $U_q[osp(2|2)]$ spin chain with central charge $c = -1$. It displays separation of spin and charge degrees of freedom in the low energy excitations with the spin part of the spectrum turning non-relativistic as $\gamma \to 2\pi$. Unlike in the antiferromagnetic regime there are no signs of a non-compact degree of freedom in the continuum limit: the zero charge sector of the low energy spectrum can be identified exactly with that of the Fateev-Zamolodchikov model in its disordered ferromagnetic phase.

In summary we have presented a comprehensive study of the critical properties of the mixed $U_q[sl(2|1)]$ superspin chain. The appearance of non-compact degrees of freedom in the continuum limit of such lattice models has been shown to be stable against deformation although it is limited to the antiferromagnetic regime of the model. As for the staggered six-vertex model studied in Ref. 6 our computation of the corresponding coupling constant (4.9) relies on the numerical solution of the Bethe equations and its derivation within an analytical approach remains an open problem. More general phases can be expected to be found when one considers mixed chains based on higher-dimensional representations of the superalgebra (and its deformation). We note, however, that already in the corresponding XXZ spin-S chains this leads to a growing number of phases (unitary and even non-unitary) as the deformation parameter is varied [26, 27, 32, 45].

Space-Time Research (QUEST).

[1] D. Serban, *Integrability and the AdS/CFT correspondence*, Habilitation, Université Paris-Sud (2010), arXiv:1003.4214.

[2] B. Kramer, T. Ohtsuki, and S. Kettemann, Phys. Rep. **417**, 211 (2005), cond-mat/0409625.

[3] H. Saleur and V. Schomerus, Nucl. Phys. B **775**, 312 (2007), hep-th/0611147.

[4] F. H. L. Essler, H. Frahm, and H. Saleur, Nucl. Phys. B **712 [FS]**, 513 (2005), cond-mat/0501197.

[5] J. L. Jacobsen and H. Saleur, Nucl. Phys. B **716**, 439 (2005), cond-mat/0502052.

[6] Y. Ikhlef, J. L. Jacobsen, and H. Saleur, Nucl. Phys. B **789**, 483 (2008), cond-mat/0612037.

[7] C. Candu, preprint(2010), arXiv:1012.0050.

[8] R. M. Gade, J. Phys. A **32**, 7071 (1999).

[9] A. B. Zamolodchikov and V. A. Fateev, Sov. J. Nucl. Phys. **32**, 298 (1980).

[10] J. L. Jacobsen, N. Read, and H. Saleur, Phys. Rev. Lett. **90**, 090601 (2003), cond-mat/0205033.

[11] W. Galleas and M. J. Martins, Nucl. Phys. B **768**, 219 (2007), hep-th/0612281.

[12] M. Chaichian and P. P. Kulish, Phys. Lett. B **234**, 72 (1990).

[13] T. Deguchi and Y. Akutsu, J. Phys. A **23**, 1861 (1990).

[14] A. J. Bracken, M. D. Gould, and R. B. Zhang, Mod. Phys. Lett. A **5**, 831 (1990).

[15] R. B. Zhang, J. Math. Phys. **33**, 1970 (1992).

[16] J. H. H. Perk and C. L. Schultz, Phys. Lett. A **84**, 407 (1981).

[17] P. P. Kulish, J. Sov. Math. **35**, 2648 (1986), [Zap. Nauch. Semin. LOMI **145**, 140 (1985)].

[18] P. P. Kulish and N. Yu. Reshetikhin, J. Phys. A **16**, L591 (1983).

[19] O. Babelon, H. J. de Vega, and C. M. Viallet, Nucl. Phys. B **200**, 266 (1982).

[20] G. A. P. Ribeiro and M. J. Martins, Nucl. Phys. B **738**, 391 (2006), nlin/0512035.

[21] F. H. L. Eßler and V. E. Korepin, Phys. Rev. B **46**, 9147 (1992).

[22] A. Foerster and M. Karowski, Nucl. Phys. B **396**, 611 (1993).

[23] M. P. Pfannmüller and H. Frahm, Nucl. Phys. B **479**, 575 (1996), cond-mat/9604082.

[24] M. P. Pfannmüller and H. Frahm, J. Phys. A **30**, L543 (1997).

[25] H. M. Babujian and A. M. Tsvelick, Nucl. Phys. B **265 [FS15]**, 24 (1986).

[26] A. N. Kirillov and N. Yu. Reshetikhin, J. Sov. Math. **35**, 2627 (1986), [Zap. Nauch. Sem. LOMI **145**, 109–133 (1985)].

[27] A. N. Kirillov and N. Yu. Reshetikhin, J. Phys. A **20**, 1565 (1987).

[28] C. S. Melo and M. J. Martins, Nucl. Phys. B **806**, 567 (2009), arXiv:0806.2404.

[29] M. Takahashi and M. Suzuki, Prog. Theor. Phys. **48**, 2187 (1972).

[30] K. Sogo, Phys. Lett. A **104**, 51 (1984).

[31] F. C. Alcaraz and M. J. Martins, J. Phys. A **22**, 1829 (1989).

[32] H. Frahm, N.-C. Yu, and M. Fowler, Nucl. Phys. B **336**, 396 (1990).

[33] F. C. Alcaraz and M. J. Martins, J. Phys. A **23**, 1439 (1990).

[34] F. C. Alcaraz and M. J. Martins, Phys. Rev. Lett. **63**, 708 (1989).

[35] N. Yu and M. Fowler, Phys. Rev. B **46**, 14583 (1992).

[36] B. Sutherland, Phys. Rev. B **12**, 3795 (1975).

[37] L. D. Faddeev and L. A. Takhtajan, Phys. Lett. A **85**, 375 (1981).

[38] F. H. L. Essler, H. Frahm, F. Göhmann, A. Klümper, and V. E. Korepin, *The One-Dimensional Hubbard Model* (Cambridge University Press, Cambridge (UK), 2005).

[39] H. J. de Vega and F. Woynarowich, Nucl. Phys. B **251**, 439 (1985).

[40] F. Woynarovich and H.-P. Eckle, J. Phys. A **20**, L443 (1987).

[41] H. J. de Vega, J. Phys. A: Math. Gen. **21**, L1089 (1988).

[42] J. Suzuki, J. Phys. A: Math. Gen. **21**, L1175 (1988).

[43] Y. Ikhlef, J. L. Jacobsen, and H. Saleur, J. Phys. A **42**, 292002 (2009), arXiv:0901.4685.

[44] J. L. Cardy, Nucl. Phys. B **270**, 186 (1986).

[45] H. Frahm and N.-C. Yu, J. Phys. A **23**, 2115 (1990).